



## 저작자표시 2.0 대한민국

이용자는 아래의 조건을 따르는 경우에 한하여 자유롭게

- 이 저작물을 복제, 배포, 전송, 전시, 공연 및 방송할 수 있습니다.
- 이차적 저작물을 작성할 수 있습니다.
- 이 저작물을 영리 목적으로 이용할 수 있습니다.

다음과 같은 조건을 따라야 합니다:



저작자표시. 귀하는 원저작자를 표시하여야 합니다.

- 귀하는, 이 저작물의 재이용이나 배포의 경우, 이 저작물에 적용된 이용허락조건을 명확하게 나타내어야 합니다.
- 저작권자로부터 별도의 허가를 받으면 이러한 조건들은 적용되지 않습니다.

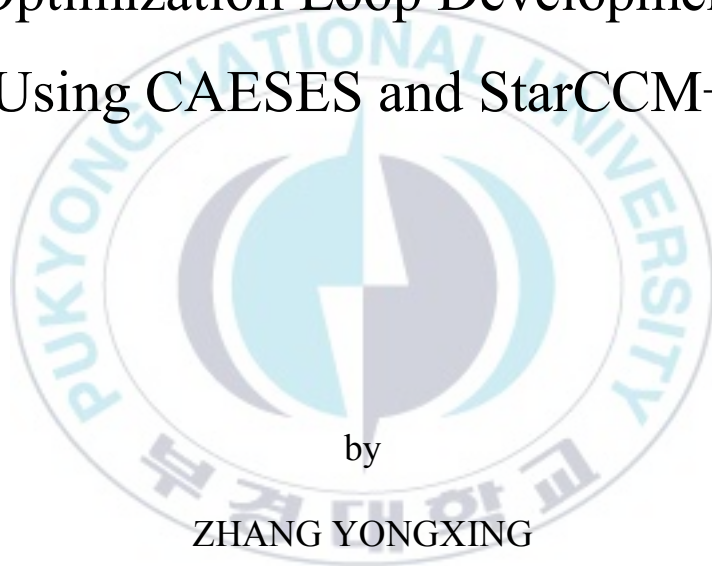
저작권법에 따른 이용자의 권리는 위의 내용에 의하여 영향을 받지 않습니다.

이것은 [이용허락규약\(Legal Code\)](#)을 이해하기 쉽게 요약한 것입니다.

[Disclaimer](#) 

Thesis for the Degree of Master of Engineering

Catamaran Bow Hull Rapid  
Optimization Loop Development  
Using CAESES and StarCCM+



by

ZHANG YONGXING

Interdisciplinary Program of Marine Convergence Design

The Graduate School

Pukyong National University

August 2019

Catamaran Bow Hull Rapid Optimization  
Loop Development Using CAESES and  
StarCCM+

CAESES 및 StarCCM+ 를 사용하여  
쌍동선 선수부분 빠른 최적화 루프

개발

Advisor: Prof. Dong Joon Kim

by

ZHANG YONGXING

A thesis submitted in partial fulfillment of the requirements  
for the degree of  
Master of Engineering  
in the Interdisciplinary Program of Marine Convergence Design  
The Graduate School  
Pukyong National University

August 2019

Catamaran Bow Hull Rapid Optimization Loop  
Development Using CAESSES and StarCCM+

A dissertation

By

ZHANG YONGXING

Approved by:



(Chairman) Prof. Joung-Hyung Cho



(Member) Prof. Jung-Min Sohn



(Member) Prof. Dong-Joon Kim

August 2019

## Contents

Abstract.....	iii
List of Figures .....	v
List of Tables.....	viii
I Introduction .....	1
1.1 Background.....	1
1.2 Overview .....	4
1.3 Outline of This Thesis .....	5
II Demi-hull Geometry Modification and Reconstruction.....	7
2.1 Free-Form Deformation (FFD) Method .....	7
2.1.1 FFD Transformation in Bulbous Bow Length.....	9
2.1.2 FFD Transformation in Bulbous Bow Breadth.....	10
2.1.3 FFD Transformation in Bulbous Bow Angle .....	11
2.2 Lackenby Method Implemented in Bow Part .....	12
III Wave Making Resistance Simulation Strategy.....	14
3.1 Theoretical Background of Wave Making Resistance Evaluation.....	15
3.2 Simulation Settings of Demi-hull.....	16
3.2.1 Domain and Boundary Condition .....	16
3.2.2 Mesh Generation Strategy .....	17
3.2.3 Results Comparison between Viscous Flow and Inviscid Flow.....	19
IV Software Integration and Demi-hull Optimization .....	24
4.1 StarCCM+ and CAESES Integration .....	24

4.2 Non-dominated Sorting Genetic Algorithm- II .....	27
4.3 Bulbous Bow Modification.....	29
4.4 Bow Part Modification .....	32
4.5 Optimization Results and Analysis .....	34
4.5.1 Bulbous Bow Optimization Results and Analysis .....	36
4.5.2 Bow Part Optimization Results and Analysis.....	40
V Distance Between Demi-hulls Optimization .....	42
5.1 Theoretical Background of Interference of Catamaran Demi-hulls .....	42
5.2 Distance Between Demi-hulls Optimization.....	44
VI Conclusion and Future Work.....	47
6.1 Conclusion .....	47
6.2 Future Work.....	48
References .....	49
국문요약.....	51
Acknowledgment.....	52
Appendix .....	53

# Catamaran Bow Hull Rapid Optimization Loop Development using CAESES and StarCCM+

ZHANG YONGXING

Department of Interdisciplinary Program of Marine Convergence Design, The  
Graduate School,  
Pukyong National University

## **Abstract**

Ship hull optimization is an iterative process, usually performed by Computer Aided Design (CAD) and Computational Fluid Dynamics (CFD) by simulating the hull form hydrodynamic performance. Researchers have been working on CAD and CFD methods to accelerate the preliminary design to make it more efficient.

CAESES is a typical CAD-CFD integration platform that will be used to manage the entire optimization process. Firstly, Lackenby method and Free-Form Deformation method was implemented to a catamaran demi-hull. The demi-hull bow hull area was modified by the change of the center of buoyancy with the displacement staying constant. Then the bulbous bow was modified in length, bulb girth and the angle between the bulbous bow and the base line. By coupling the CFD solver StarCCM+ with CAESES, the wave making resistance and wave pattern of the demi-hull in calm water was simulated and optimized by

Non-dominated Sorting Genetic Algorithm (NSGA)-II. Finally, after getting the optimal demi-hull, the distance between the two demi-hull was optimized.

Inviscid fluid model in RANS method was used to reduce the computing time while ensuring the accuracy in the simulations. Results show that this optimization loop can be used to reduce the wave making resistance of catamaran in calm water.

**Keywords:** Catamaran, Free-Form Deformation, Lackenby, Wave making resistance, Optimization



## List of Figures

Fig. 2.1 Bulbous bow model and the FFD control box and control points .....	8
Fig. 2.2 FFD transformation in bulbous bow length.....	9
Fig. 2.3 FFD transformation in bulbous bow breadth.....	10
Fig. 2.4 FFD transformation in bulbous bow angle.....	11
Fig. 2.5 Translation of stations with Lackenby method.....	12
Fig. 2.6 Lackenby method implemented in the bow part.....	13
Fig.3.1 Domain and boundary condition side view .....	16
Fig.3.2 Domain and boundary condition top view .....	17
Fig.3.3 Subtracted object.....	17
Fig.3.4 Volumetric control blocks in mesh generation.....	18
Fig.3.5 Mesh generation results.....	18
Fig.3.6 Sectional view of mesh generation results .....	19
Fig.3.7 Convergence history comparison between viscous flow and inviscid flow at $F_n=0.36$ .....	20
Fig.3.8 Convergence history comparison between viscous flow and inviscid flow at $F_n=0.55$ .....	20
Fig.3.9 Convergence history comparison between viscous flow and inviscid flow at $F_n=0.73$ .....	21
Fig.3.10 Convergence history comparison between viscous flow and inviscid flow at $F_n=0.92$ .....	21
Fig.3.11 Wave pattern comparison between Inviscid flow(left) and Viscous flow(right) at $F_n=0.36$ .....	22

Fig.3.12 Wave pattern comparison between Inviscid flow(left) and Viscous flow(right) at $Fn=0.55$ .....	22
Fig.3.13 Wave pattern comparison between Inviscid flow(left) and Viscous flow(right) at $Fn=0.73$ .....	23
Fig.3.14 Wave pattern comparison between Inviscid flow(left) and Viscous flow(right) at $Fn=0.92$ .....	23
Fig.4.1 StarCCM+ and CAESES connection flow chart .....	26
Fig.4.2 Software connector interface in CAESES .....	27
Fig.4.3 Generic algorithm working process flow chart.....	28
Fig.4.4 NSGA- II algorithm working process flow chart in this study.....	29
Fig.4.5 Bulbous bow length constraints ( $-0.02*LOA \leq \Delta L \leq 0.02*LOA$ ) .....	30
Fig.4.6 Bulbous bow breadth constraints ( $0.8*B \leq B' \leq 1.3*B$ ) .....	31
Fig.4.7 Bulbous bow angle constraints ( $-9^\circ \leq \alpha \leq 3^\circ$ ) .....	32
Fig.4.8 Bow part LCB moving forward by 0.4% .....	33
Fig.4.9 Bow part LCB moving backward by 0.4%.....	34
Fig.4.10 Demi-hull optimization loop flow chart in this study .....	34
Fig.4.11 Wave making resistance of 200 different bulbous bow plans .....	36
Fig.4.12 Wave making resistance of 5 generations of different bulbous bow plans	37
Fig.4.13 Length evolution trend of 5 generations of different bulbous bow plans..	38
Fig.4.14 Breadth evolution trend of 5 generations of different bulbous bow plans.	38
Fig.4.15 Angle evolution trend of 5 generations of different bulbous bow plans ...	39
Fig.4.16 Optimal bulbous bow No.1 (red) and No.2 (blue) profile .....	40
Fig.4.17 $R_w$ for different bow part plans at $Fn=0.73$ .....	41

Fig.5.1 The effect of demi-hull separation on catamaran resistance at different  $F_n$  [Millward (1992)] ..... 43

Fig.5.2 The  $R_w$  of catamaran resistance at different separation plans..... 45

Fig.5.3 The  $R_w$  difference of catamaran and two demi-hulls at different separation plans ..... 45



## List of Tables

Table 3.1 Main data of the demi-hull.....	15
Table 4.1 Comparison of optimal bulbous bows from two optimization process ...	37



# I Introduction

## 1.1 Background

Simulation-driven Design (SDD) is one of the most important methods for ship optimization design. With the development of computer-aided design technologies, the hull shape optimization research through computer simulation has been gradually gain popularity in designing more energy-saving and environmentally friendly ships. In the preliminary design stage of the ship design process, the optimization of the hydrodynamic characteristics of the hull form plays an extremely important role. As the processing speed of computers speed up and hardware characteristics improve, researchers began to experiment with Computer Aided Design (CAD) and simulation (CFD) methods. This integration scheme has proved to be successful in the field of structural mechanics. However, since the calculation of fluid dynamics is highly dependent on the geometry model and the amount of data to calculate is huge, this integration scheme has not been fully implemented in the field of fluid dynamics.

Lei Li et al. combined simulation intent and design intent, achieving good results in the case of the steam assisted gravity drainage (SAGD) outflow control device (OCD) in 2016. Fluid physics and dynamic physics are proposed to convey the simulation intent to help input data processing and generate a more stable design, achieving semi-automation of optimized design cycles and take CAD/CFD integration to a higher level. B. Sener Focus on the fully parametric design process

for frigate type surface combatant. By Taking use of CAESES (a unique CAD - CFD integration platform) to create a fully parameterized model from a set of parameters and connect to a CFD solver. Shenglong Zhang et al. developed an improved particle swarm optimization (IPSO) algorithm and using the arbitrary shape deformation (ASD) technique. It is able to change the shape of the geometry.

Due to the complex geometry shape of the hull, it is difficult to use a numerical method to describe it. Researchers often choose to modify the hull form by making changes on the mother ship. In 1950, Lackenby developed a method to modify the hull by controlling the position of the center of buoyancy, shifting the section curves of the mother ship. Since then, Lackenby method has been widely used in hull modification. Karria and Krishna (2010) used the Lackenby method to modify the hull and used the Panel method to optimize the hull shape. By writing Python code, an optimization loop was developed to reduce the hull form optimization cycle.

The wave making resistance of a ship hull depends largely on the bow part (between the stem and mid-ship). It is efficient to optimize the bow part of a ship for reducing the wave making resistance. Bulbous bow and the hull between bulbous bow and mid-ship are two main objects recommended to be optimized.

Recently, researchers consider two main ways to modify the bulbous bow geometry shape: parametric modeling and Free-Form Deformation. Chrismianto and Kim (2014) used the cubic Bezier curve and curve-plan intersection method to generate the parametric bulbous bow. Luo and Lan (2016) used B-Spline curve and

NURBS curve to generate the parametric bulbous bow in CAESES. Also, the plug-in software named Grasshopper was used to generate the parametric bulbous bow from a few vertexes and NURBS curves.

Free-Form Deformation method was first proposed by Sederberg and Parry in 1986 and it has been widely used in hull form modification. Wu et al. (2017) implemented the shifting method to modify the hull geometry form globally and FFD method to modify the hull locally. Coppédé et al. (2018) combined subdivision surface and FFD method modified bulbous bow. FFD method was used in volume control and the subdivision surface was used in polygon control.

Different governing equations in CFD solver were used to predict ship hull hydrodynamic performance in recent years. One of the most popular ways is Reynolds averaged Navier–Stokes (RANS) method. Tezdogan et al. (2018) implemented RANS-VOF solver to simulate total resistance of the ship in calm water. Sinkage and trim of a fishing vessel in calm water was set to be the objective function during the hydrodynamic optimization process. Zhang et al. (2018) used RANS method to calculate the total resistance during the optimization framework.

Usually, hundreds of simulations are required to perform a whole optimization process, Because of this the hydrodynamic performance prediction can be quite time taking. Researchers have tried different ways to reduce computing time. Wu et al. (2017) used the kriging method to calculate the total resistance to reduce the computing time first and then used Neumann-Kelvin method, RANS method to verify the result. Cheng et al. (2018) selected the potential flow theory to perform

CFD analysis. Han et al. (2012) selected non-linear potential flow using Rankine panels method to predict trim and sink during the simulation. Kostas et al. (2018) employed Neumann-Kelvin formulation and boundary element method (BEM) simulating the wave making resistance.

To find a fast, accurate and optimal solution, many kinds of optimization equations were implemented in the whole optimization process (which process are you talking about). Zhang et al. selected Particle Swarm Optimization (PSO) algorithm in order to find the optimal bulbous bow. Huang et al. implemented a new improved Artificial Bee Colony algorithm (NIABC) in KCS hull optimization.

## 1.2 Overview

Researchers have been working on coupling CAD and CFD and optimization algorithms to accelerate the preliminary design to make it more efficient. High-speed Catamaran travels with high Froude number ( $F_n > 0.3$ ) and wave making resistance usually take a large portion of the total resistance ( $R_w > 50\%R_t$ ). Ship hull form between the stem and the mid-ship affect the wave making resistance performance significantly.

In this study, wave making resistance of catamaran in calm water was selected to be the object function in the whole optimization process. Catamaran demi-hulls' wave making resistance performance in calm water was optimized first and then the distance between demi-hulls was optimized. The optimization process is listed below:

1. Free-Form Deformation (FFD) method was employed to modify the bulbous bow shape with the design variables: length, breadth, and angle(between bulbous bow and baseline).

2. Coupling CAD and CFD solver(CAESSES and StarCCM+), 200 simulations were carried out and compared to get the optimal bulbous bow No.1

3. Optimization method: Non-dominated Sorting Genetic Algorithm (NSGA)-II was employed to get optimal bulbous bow No.2.

4. Comparing optimal bulbous bow No.1 and No.2, get a final bulbous bow.

5. The bow part between bulbous bow and mid-ship was modified by using the Lackenby method (shifting the section curve) design variable: Longitudinal Centre of Buoyancy(LCB).

6. 9 different plans from Lackenby method were computed and an optimized demi-hull form was obtained.

7. Finally, the distance between catamaran demi-hulls was optimized and the final optimal catamaran plan was obtained.

### **1.3 Outline of This Thesis**

The present study consists of 6 chapters, a brief description of these chapters are summarized next:

Chapter I, Introduction presents the background in which this study was founded, and includes several overviews of related literature in ship hull optimization.

Chapter II, Demi-hull Geometry Modification and Reconstruction presents the CAD part work and methodology of this study. The geometry variation method is presented in detail.

Chapter III, Wave Making Resistance Simulation Strategy presents the theory and usage of CFD solver StarCCM+. Then inviscid flow results and viscous flow results at different  $F_n$  was compared in this chapter.

Chapter IV, Software Integration and Demi-hull Optimization presents the demi-hull optimization process under the framework of CAESES and StarCCM+ integration.

Chapter V, Distance Between Demi-hulls Optimization presents the theoretical background and optimization of the distance between two demi-hulls.

Chapter VI, Conclusion and Future Work presents a brief summary and final conclusion of this thesis. Disadvantages and future work was also discussed in this chapter.

## **II Demi-hull Geometry Modification and Reconstruction**

Due to the complex geometry shape of the hull, it is difficult to use a numerical method to describe the hull. In recent years, there are two main popular ways to modify the bulbous bow geometry shape: parametric modeling method and mother ship transformation method. Since it is quite difficult to describe the demi-hull accurately by parametric modeling method, the mother ship transformation method was selected to complete the hull geometry modification and reconstruction.

In this research, Free-Form Deformation (FFD) method and Lackenby method were implemented to the bulbous bow and bow part between the bulbous bow and mid-ship respectively.

### **2.1 Free-Form Deformation (FFD) Method**

Free-Form Deformation (FFD) method was implemented to the demi-hull bulbous bow. Free-form deformation method (FFD) is proposed based on the idea of enclosing an object within a control cube with control points on it. And transforming the hull as the cube is deformed. Deformation of the hull is based on the concept of so-called hyper-patches, which are three-dimensional of parametric curves such as Bezier curves, B-splines, or NURBS. In this research, the bulbous

bow was modified in three dimensions, including length, breadth, and angle between the bulbous bow and baseline.

Fig.2.1 shows the original bulbous bow model and the FFD control box and control points. The bulbous bow will be transformed by the transformation of the control box, and the control box transforms along with the control points. There are total 80 control points and several of them were defined to transform in a certain way. In Fig.2.1, the yellow control points are the defined control points which are allowed to transform. The way that FFD method works in this way: combine the bulbous bow model and the control box together, as the control points transform in a certain way, the control box will transform so the bulbous bow model will transform along with the control box. More detail explanation of each dimension will be introduced later.

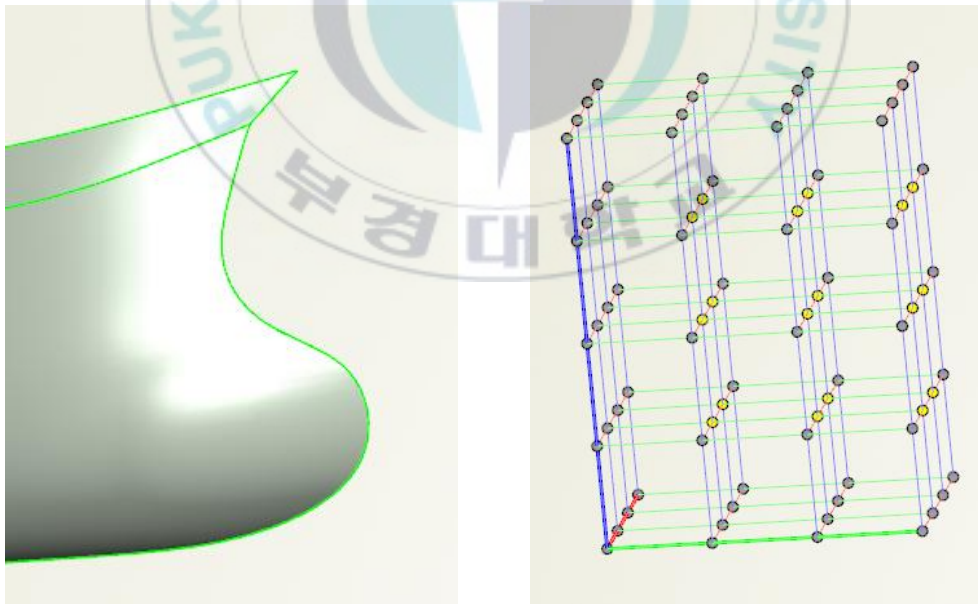


Fig. 2.1 Bulbous bow model and the FFD control box and control points

### 2.1.1 FFD Transformation in Bulbous Bow Length

Fig. 2.2 is bulbous bow transform in the length by FFD method. The yellow control points in the control box were defined to move forward in the x-direction which means the bulbous bow will also be transformed to be longer. The surface of the hull model was generated in mesh so the model will keep watertight while transforming. FFD method allowed the surface mesh modifying smoothly as it is shown in Fig. 2.2.

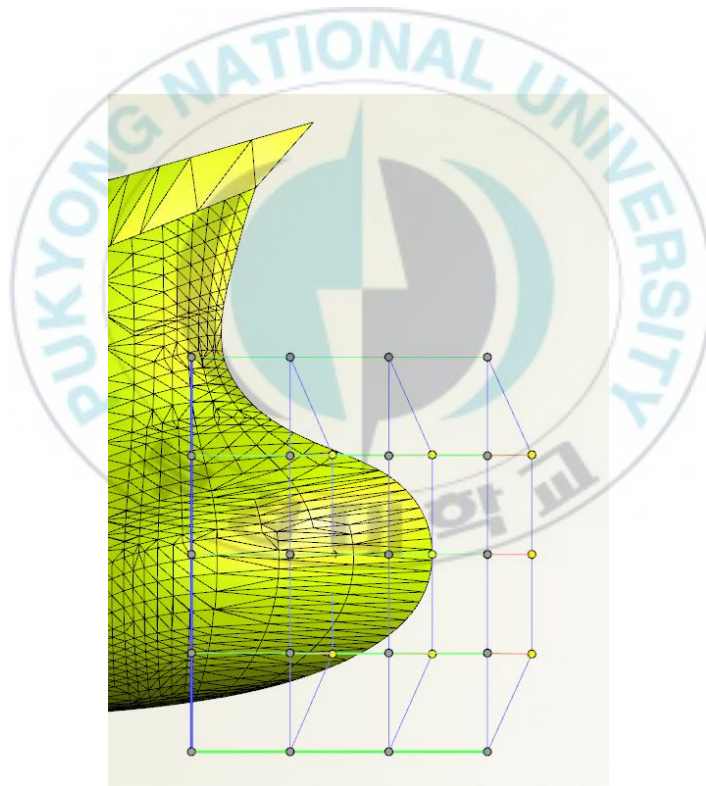


Fig. 2.2 FFD transformation in bulbous bow length

### 2.1.2 FFD Transformation in Bulbous Bow Breadth

Fig. 2.3 is bulbous bow transform in the breadth by FFD method. The control points on the edge of the control box were defined to expand in the y-direction which means the bulbous bow will also be transformed to be wider.

The control points were defined to expand in a different degree in this case. As can be seen in Fig. 2.3, the front of bulbous bow expand relatively wider because of the bulbous bow's original shape characteristics. FFD method allowed the surface mesh modifying smoothly as it is shown in Fig. 2.3.

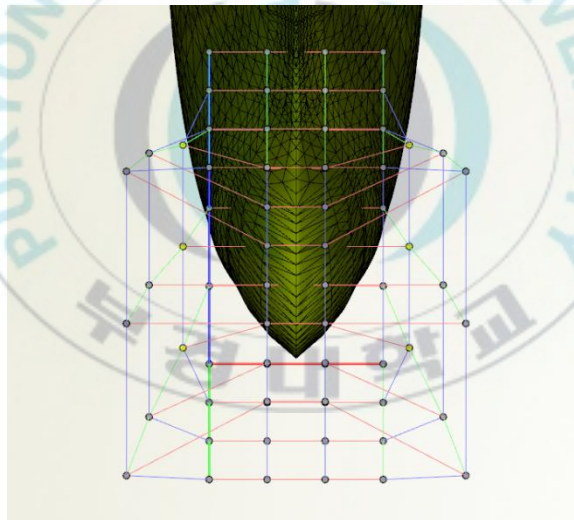


Fig. 2.3 FFD transformation in bulbous bow breadth

### 2.1.3 FFD Transformation in Bulbous Bow Angle

Fig. 2.4 is bulbous bow transform in the angle by FFD method. Angle means the angle between bulbous bow keel line and baseline. The control points on the control box were defined to rotate by the y-axis. The shape of the bulbous bow will also be modified by angle.

The control points were defined to expend in a different degree in this case. As can be seen in Fig. 2.4, the front of the bulbous bow was defined to rotate in a bigger angle relatively because of the bulbous bow's original shape characteristics. The surface of the hull model was generated in mesh so the model will keep watertight while transforming. FFD method allowed the surface mesh modifying smoothly as it is shown in Fig. 2.4.

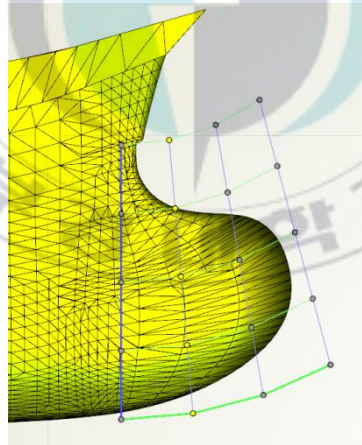


Fig. 2.4 FFD transformation in bulbous bow angle

## 2.2 Lackenby Method Implemented in Bow Part

The lackenby method is a method to modify the hull by controlling the position of the center of buoyancy, shifting the section curves of the mother ship. Lackenby allows the reconstructed ship hull keeping the displacement to be constant.

Fig. 2.5 shows the translation of stations with Lackenby method. There are 5 main procedures in Lackenby method:

1. determine the curve of area versus stations abscissa,  $a=A(x)$ .
2. determine the LCB abscissa and  $\psi$ .
3. using the required new location  $B'$  for the buoyancy center, determine the angle
4. move all points  $(a, x)$  of the curve areas horizontally to  $(a, x+\arctan(\alpha))$ .
5. calculate the new center of buoyancy  $B^*$ , and check if  $B^*=B'$  (within an acceptable margin of error), otherwise repeat the preceding procedure.

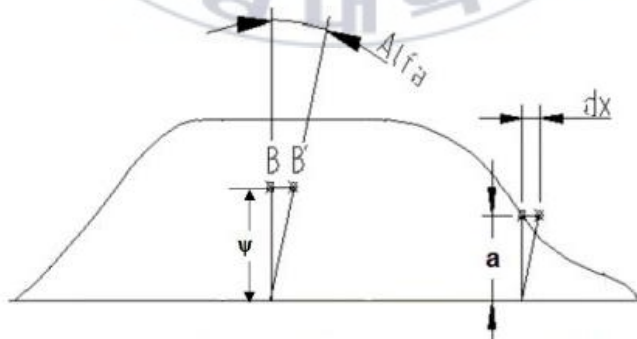


Fig. 2.5 Translation of stations with Lackenby method

As it is shown in Fig. 2.5, the original Lackenby method works based on the sectional area curve and it modifies the ship hull form in a global scope. The ship hull was divided into two parts: bow and stern by the mid-ship section. In this way, the hull form changes in a big range and the center of buoyancy of the ship moves in a big amount. It is considered to be having a negative impact on the statics performance. In this study, the Lackenby method was implemented only in the bow part (between mid-ship and bulbous bow).

Fig. 2.6 shows Lackenby method implemented in the bow part. Because the bulbous bow will be modified by the FFD method, the Lackenby method will be implemented in the bow part as it is shown in Fig. 2.6. 50 section curves were calculated to get the sectional area curve. There are two sectional area curves in the figure, one is the original sectional curve and another one is the new sectional area curve from the modified hull form.

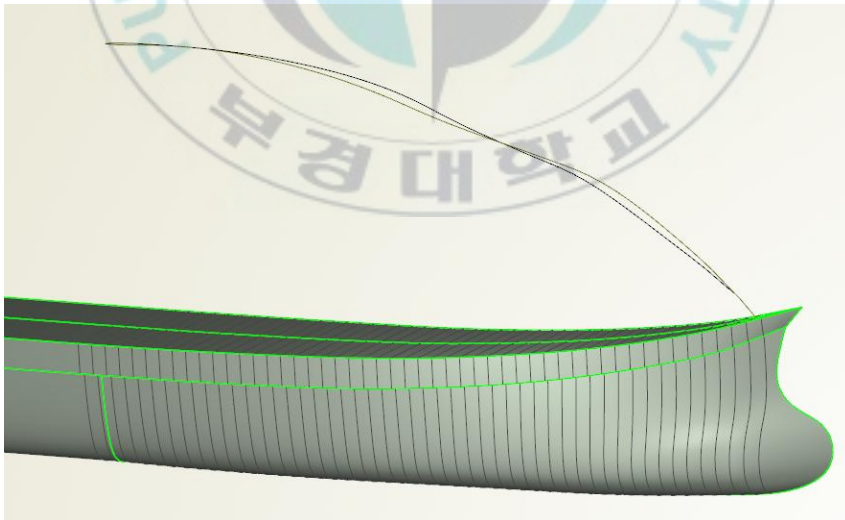


Fig. 2.6 Lackenby method implemented in the bow part

### III Wave Making Resistance Simulation

#### Strategy

High-speed Catamaran travels with high Froude number ( $F_n > 0.3$ ) and wave making resistance usually take a large proportion of total resistance ( $R_w > 50\%R_t$ ). So optimizing the wave making resistance is an effective way for high-speed ship hull resistance performance optimization.

The wave making the resistance of a catamaran is the object function of the whole optimization process. StarCCM+ was selected to perform the wave making resistance simulation and evaluation. STAR-CCM+ is a CFD solver for simulating products and designs that operate under real-world conditions. STAR-CCM+ brings automation design exploration and optimization to each engineer's simulation toolkit, enabling engineers to effectively explore the entire design space instead of focusing on single point design.

A high-speed catamaran was selected to optimize in this study. The main data of this catamaran demi-hull is showed in Table 3.1.

Table 3.1 Main data of the demi-hull

LOA	21.7 (m)
L <sub>pp</sub>	20.0 (m)
B	2.5 (m)
D	3.2 (m)
d	1.6 (m)
V	20 (knot)
Fn	0.73

### 3.1 Theoretical Background of Wave Making Resistance Evaluation

The CFD solver STAR-CCM+ uses the finite volume method and Reynolds-averaged Navier–Stokes (RANS) equations as the governing equation. Since the wave making resistance is based on the concept of considering the fluid model with no impact of turbulence and the fluid model is inviscid. During the simulation in STAR-CCM+, the fluid model physics setting part will be set as inviscid. This allows evaluating the wave making resistance accurately and efficiently. Because the results show that the computing time reduces for 60 percent compared to the simulation with the viscous flow. And the simulation results have

no big difference between them. The comparison will be explained in the later section.

## 3.2 Simulation Settings of Demi-hull

### 3.2.1 Domain and Boundary Condition

The computational domain was built as a rectangular block. Like the towing tank in the ship model experimental tank, the domain was set as it is shown in Fig.3.1 and Fig.3.2. The Length between perpendicular of the demi-hull was noted as  $L$ . The length in front of the hull was set as  $1.2L$  and the length from the stern to outlet boundary was set as  $2.4L$ . The breadth between the symmetry and the wall was set as  $1.2L$ .



Fig.3.1 Domain and boundary condition side view

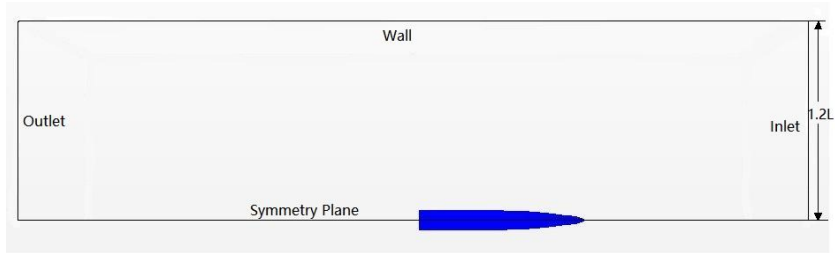


Fig.3.2 Domain and boundary condition top view

### 3.2.2 Mesh Generation Strategy

To generate the mesh of the whole computing domain, the object of ship hull and the towing tank should be operated to be one object. Using the function subtract in StarCCM+, these two objects became one object as it is shown in Fig.3.3.

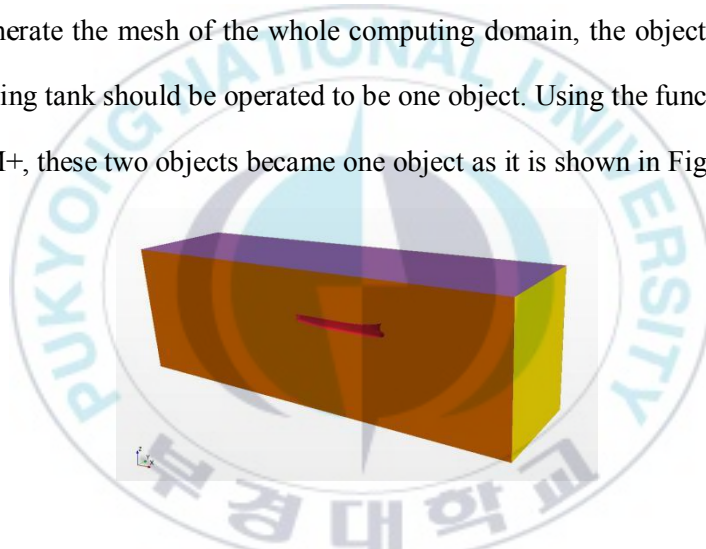


Fig.3.3 Subtracted object

The mesh size was controlled by 4 blocks as it is shown in Fig.3.4. The meshes around the free surface and bow area were set to be generated relatively specific and small so that the computing results will converge faster and better.

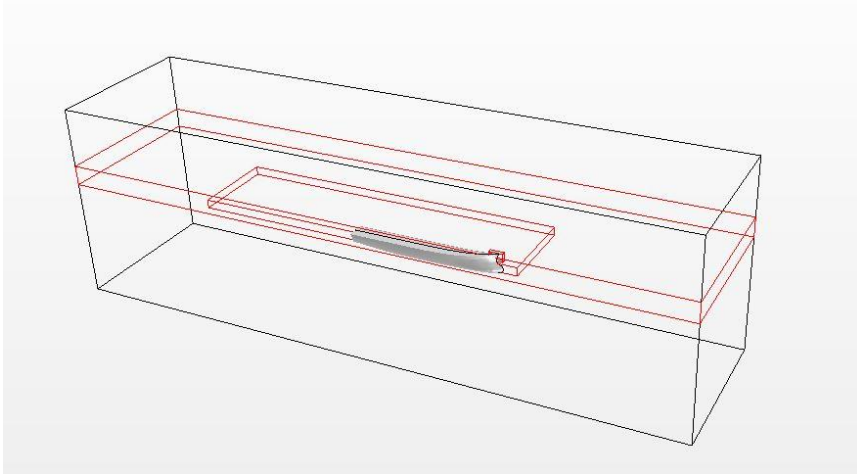


Fig.3.4 Volumetric control blocks in mesh generation

For mesh generation, the  $Z$  direction was generated to be relatively thin around the free surface. The  $X$  and  $Y$  directions are relatively wide. Fig.3.5 and Fig.3.6 show the mesh generated in the simulation.

The mesh distribution can ensure the calculation's accuracy with fewer cells number. total mesh cells number is around 340000.

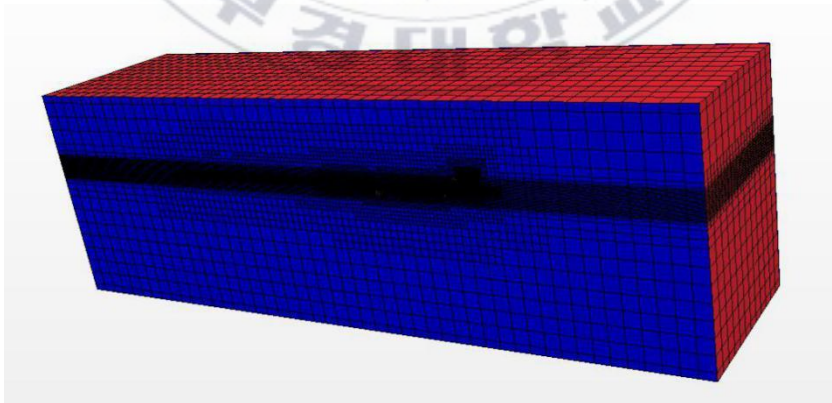


Fig.3.5 Mesh generation results

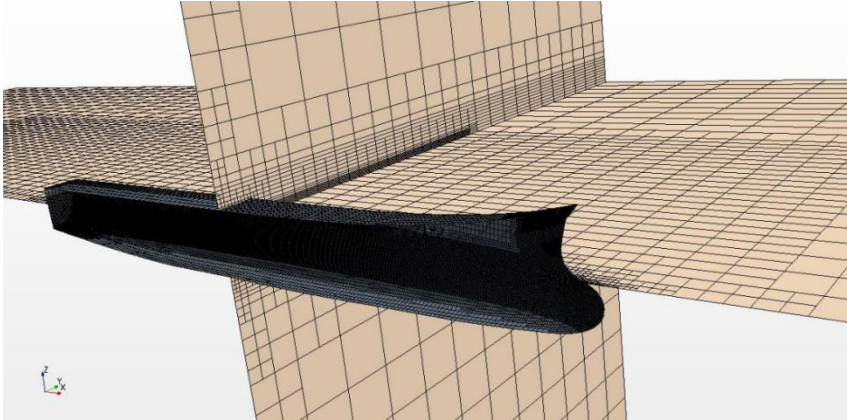


Fig.3.6 Sectional view of mesh generation results

### 3.2.3 Results Comparison between Viscous Flow and Inviscid Flow

To evaluate the wave making resistance of a ship, the fluid model was set to be the inviscid fluid model. The simulation results of demi-hull between viscous flow and inviscid flow will be compared in this section to verify the inviscid flow can be used in wave making resistance prediction. The demi-hull was simulated in different Froude number (Fn).

Fig.3.7~Fig.3.10 show the convergence history comparison between viscous flow and inviscid flow at different Fn. The differences between viscous flow and inviscid flow are less than 1 percent. Comparison results show that inviscid flow can be implemented in wave making resistance simulation of catamaran demi-hull.

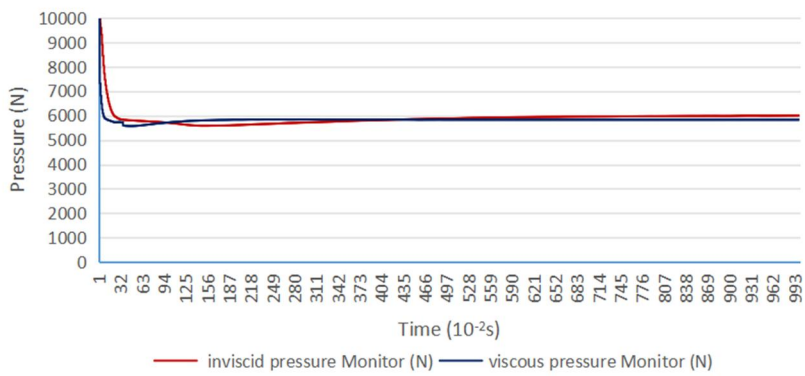


Fig.3.7 Convergence history comparison between viscous flow and inviscid flow at  $Fn=0.36$

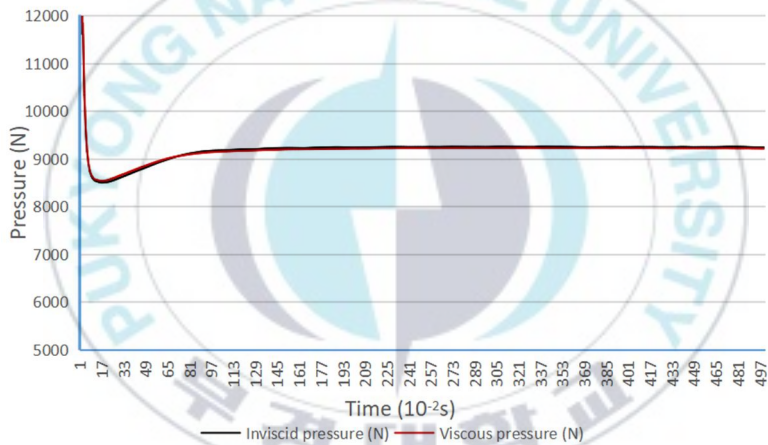


Fig.3.8 Convergence history comparison between viscous flow and inviscid flow at  $Fn=0.55$

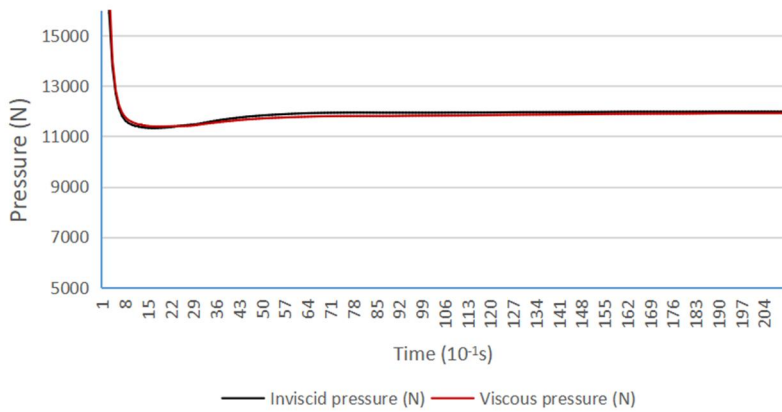


Fig.3.9 Convergence history comparison between viscous flow and inviscid flow at  $F_n=0.73$

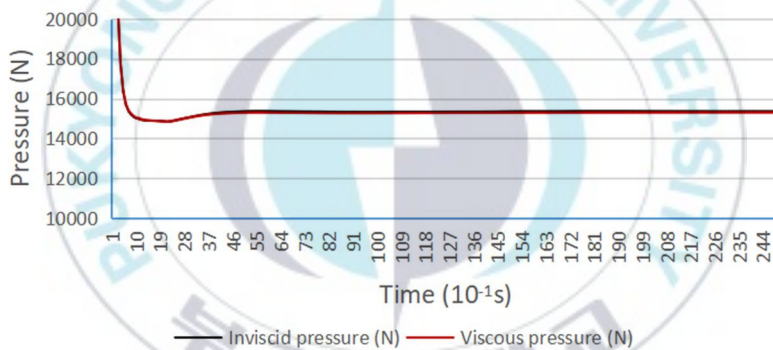


Fig.3.10 Convergence history comparison between viscous flow and inviscid flow at  $F_n=0.92$

Fig.3.11~Fig.3.14 show wave pattern comparison between inviscid flow and viscous flow at different  $F_n$ . The results show that it is feasible to use the inviscid fluid model to simulate wave making resistance of the demi-hull.

The computing time reduces about 60% by using inviscid fluid model. (CPU 2core, Inviscid: 1.5h; Viscous 3h)

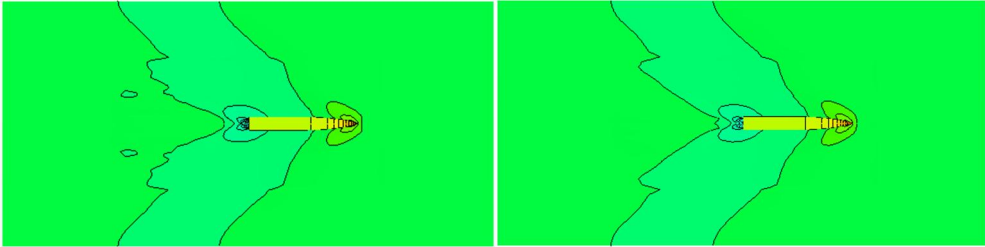


Fig.3.11 Wave pattern comparison between Inviscid flow(left) and Viscous flow(right) at  $F_n=0.36$

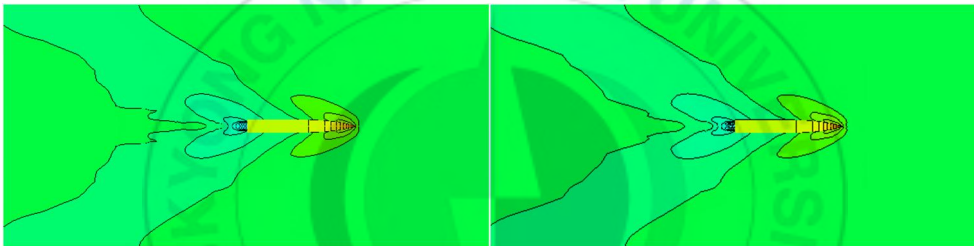


Fig.3.12 Wave pattern comparison between Inviscid flow(left) and Viscous flow(right) at  $F_n=0.55$

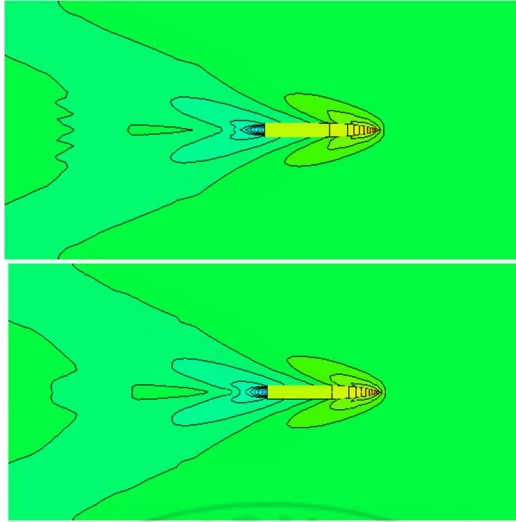


Fig.3.13 Wave pattern comparison between Inviscid flow(left) and Viscous flow(right) at  $F_n=0.73$

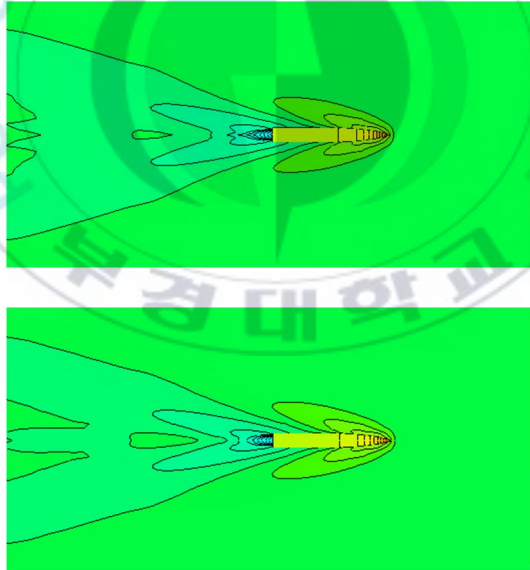
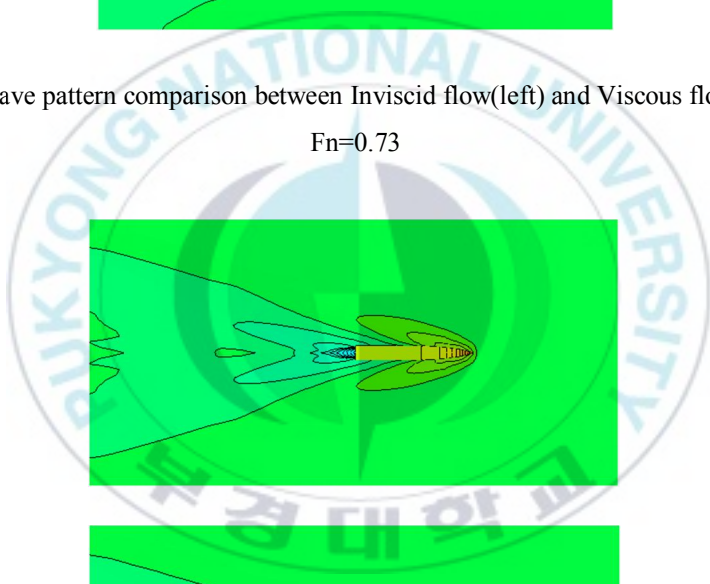


Fig.3.14 Wave pattern comparison between Inviscid flow(left) and Viscous flow(right) at  $F_n=0.92$

# IV Software Integration and Demi-hull Optimization

By coupling the CFD software StarCCM+ and CAESES, the wave making resistance was simulated in StarCCM+ and feedback to CAESES. Firstly, Free-Form Deformation (FFD) method was employed to modify the bulbous bow shape with the design variables: length, breadth, and angle(between bulbous bow and baseline). Then Optimization Algorithm: Non-dominated Sorting Genetic Algorithm (NSGA)-II was employed to get the optimal bulbous bow. Then the bow part between bulbous bow and mid-ship was modified by Lackenby method (shifting the section curve) design variable: Change of Longitudinal Centre of Buoyancy ( $\Delta LCB$ ). 9 different plans from Lackenby method were computed and the optimized Demi-hull form was obtained.

## 4.1 StarCCM+ and CAESES Integration

CAESES is an integration platform that can launch and control CFD runs or any other simulation processes. CAESES itself has no simulation solver such as CFD tools to create a closed loop. Moreover, it can be used as a Post Processing GUI (graphical user interface) for any external software. Basically, any external tool that can be run in batch mode can be coupled in just a few minutes. In here, CFD solver is coupled but any other CAE or preliminary design tool coupling can be possible – the entire data exchange and management are controlled by CAESES.

The performance function within the CAESES are:

- Export of geometry using common CAD formats (e.g. IGES, STEP, ACIS, various STL formats) automatically to black box solver.
- Easy definition of geometry using the Feature Definition function.
- Post-Processing visualization capability ( GUI)
- Result value from the CFD can extract easily.
- Coupling of multiple external tools and setting up sequential process chains, e.g. meshing > simulation 1 > simulation 2 > ... > post processing

Fig.4.1 shows the flow chart of StarCCM+ and CAESES connection process.

NSGA is one of optimization equation with the full name Non-dominated Sorting Genetic Algorithm. It will help in finding the optimal solution more efficient and more accurate. With the NSGA operator in the CAESES, different design variables will be generated so different hull form plans will be obtained. Then the different hull form plans will be exported to StarCCM+ as STL file. Every hull form plans will be simulated and evaluated by StarCCM+ in wave making resistance. This process will repeat until the wave making resistance converge in a certain range.

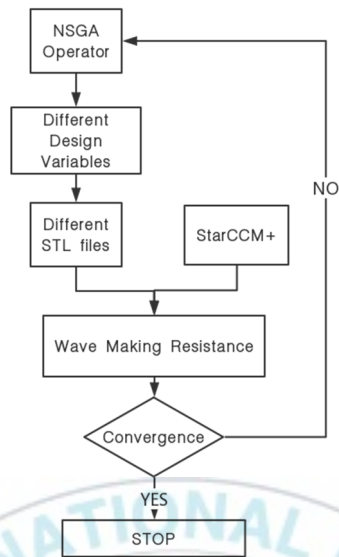


Fig.4.1 StarCCM+ and CAESES connection flow chart

Fig.4.2 Shows the software connector interface in CAESES. The input geometry is STL file from NSGA, the input file is SIM file and Macro file recorded from StarCCM+, the result value is from the post-processing file.



Fig.4.2 Software connector interface in CAESES

## 4.2 Non-dominated Sorting Genetic Algorithm- II

Non-dominated Sorting Genetic Algorithm-II (NSGA-II) is an extension of the genetic algorithm. It will help in finding the optimal solution more efficient and more accurate.

The objective of the NSGA-II algorithm is to improve the adaptive fit of a population of candidate solutions to a Pareto front constrained by a set of objective functions. The algorithm uses an evolutionary process with surrogates for evolutionary operators including selection, genetic crossover, and genetic mutation.

The population is sorted into a hierarchy of subpopulations based on the ordering of Pareto dominance. The similarity between members of each sub-group is evaluated on the Pareto front, and the resulting groups and similarity measures are used to promote a diverse front of non-dominated solutions. Fig.4.3 shows the flow chart of the generic algorithm working process.

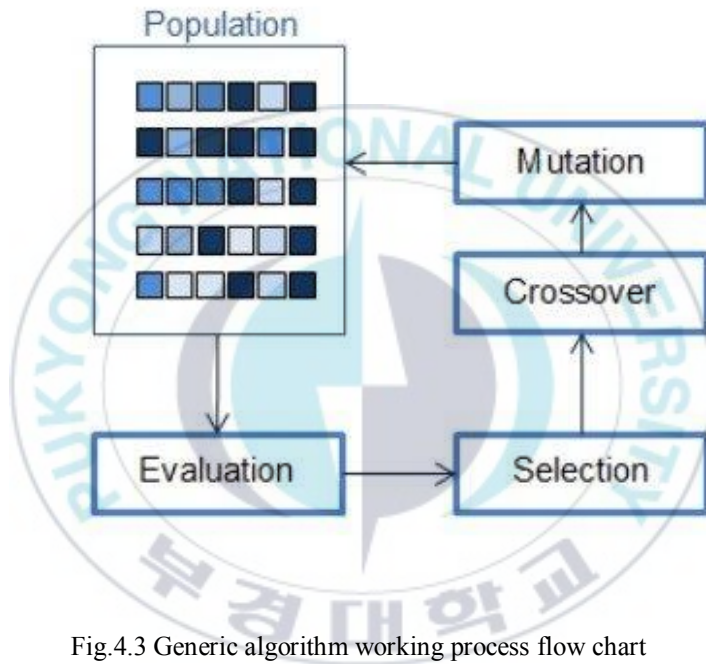


Fig.4.3 Generic algorithm working process flow chart

Fig.4.4 shows the flow chart of NSGA-II algorithm working process. Firstly, 27 initial design plans will be generated as the first generation. And 27 simulations will be carried in StarCCM+ getting the results of wave making resistance. The well-performed plans will be selected to mutate and crossover to get the new generation. The simulations and selection will repeat until the results of wave making resistance converge. Finally, the optimal hull form will be obtained.

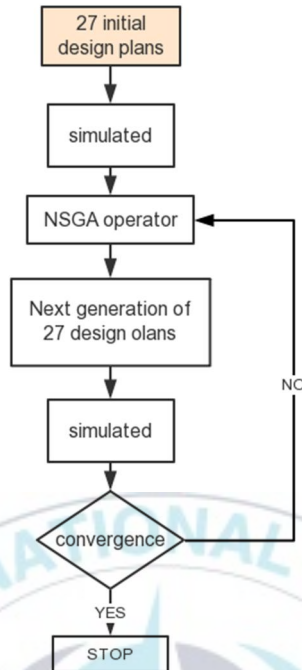


Fig.4.4 NSGA- II algorithm working process flow chart in this study

### 4.3 Bulbous Bow Modification

Free-Form Deformation (FFD) method was implemented to the demi-hull bulbous bow. In this research, the bulbous bow was modified in three dimensions, including length, breadth and angle between the bulbous bow and baseline.

Fig.4.5 shows the length of catamaran demi-hull bulbous bow modified under the constraints of  $-0.02 \cdot L_{OA} \leq \Delta L \leq 0.02 \cdot L_{OA}$ . where the  $\Delta L$  means the change of the length of the bulbous bow, the  $L_{OA}$  means length overall.

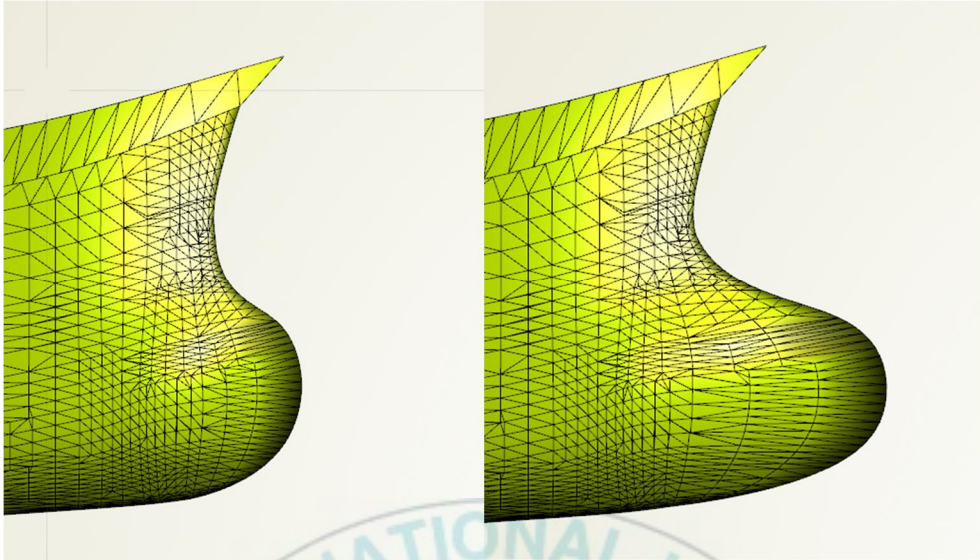


Fig.4.5 Bulbous bow length constraints ( $-0.02*LOA \leq \Delta L \leq 0.02*LOA$  )

It can be seen that the surface of the hull is generated by mesh, this makes the hull is watertight and the surface of the hull can remain smooth while the bulbous bow was modified by FFD method.

Fig.4.6 shows the breadth of catamaran demi-hull bulbous bow modified under the constraints of  $0.8*B \leq B' \leq 1.3*B$  where the B means the original breadth of the bulbous bow, the B' means length overall. It can be seen that the surface of the hull is generated by mesh, this makes the hull is watertight and the surface of the hull can remain smooth while the bulbous bow was modified by FFD method.

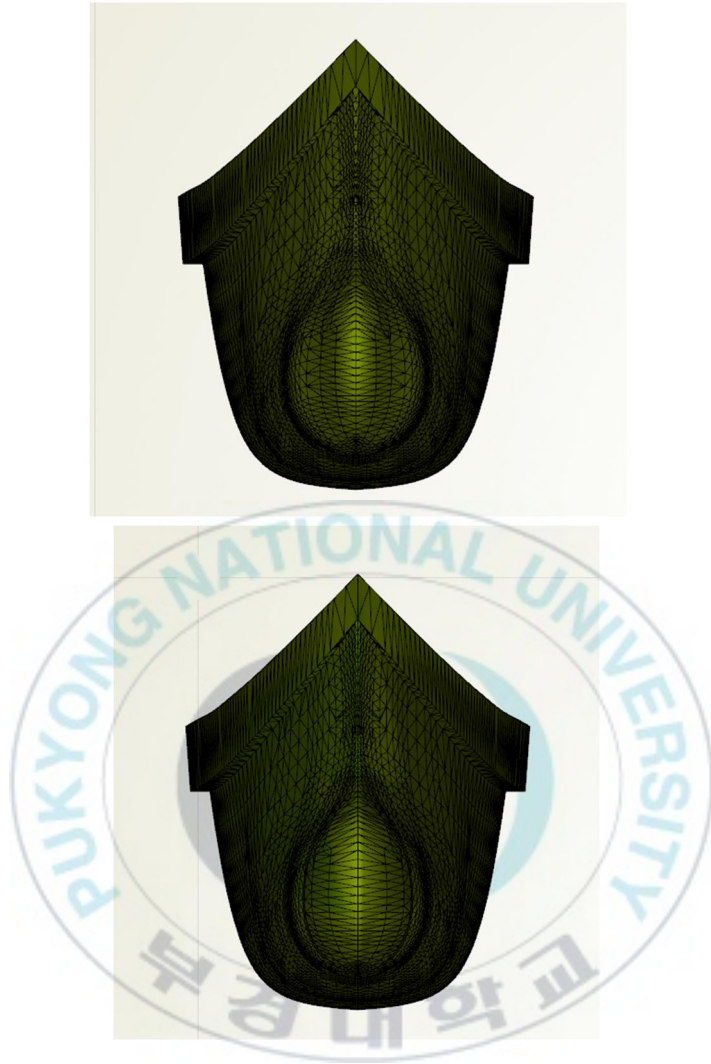


Fig.4.6 Bulbous bow breadth constraints ( $0.8*B \leq B' \leq 1.3*B$ )

Fig.4.7 shows the breadth of catamaran demi-hull bulbous bow modified under the constraints of  $-9^\circ \leq \alpha \leq 3^\circ$  where the  $\alpha$  means the original breadth of the bulbous bow, the  $B'$  means length overall.

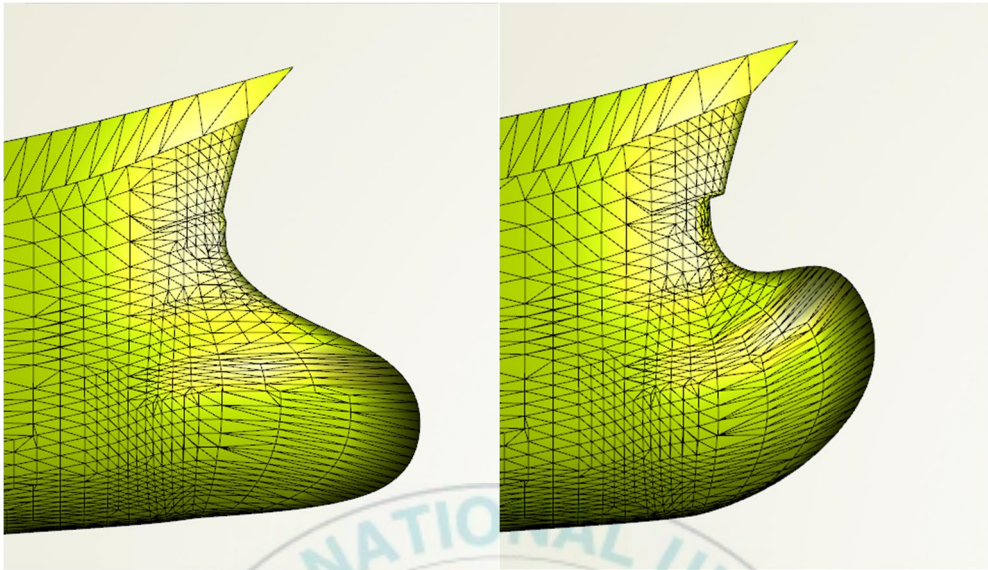


Fig.4.7 Bulbous bow angle constraints ( $-9^{\circ} \leq \alpha \leq 3^{\circ}$ )

The operating cubic in FFD method was set as relatively big so the gap between the bulbous bow and the main hull will be beyond of the waterline making sure that the simulation cannot be affected by the gap.

#### 4.4 Bow Part Modification

The bow part means the hull part between the bulbous bow and mid-ship. As it was mentioned before, the bow part was modified by Lackenby method. Lackenby method was implemented in the bow part so the hull form will be modified while keeping the displacement being constant. The longitudinal center of buoyancy (LCB) will change slightly and the change of the longitudinal center of buoyancy ( $\Delta LCB$ ) was set to be the design variables.

Fig.4.8 shows the bow part of catamaran demi-hull modified under the constraints of LCB moving forward by 0.4%, the design variables will be  $\Delta\text{LCB}=0.4$ .

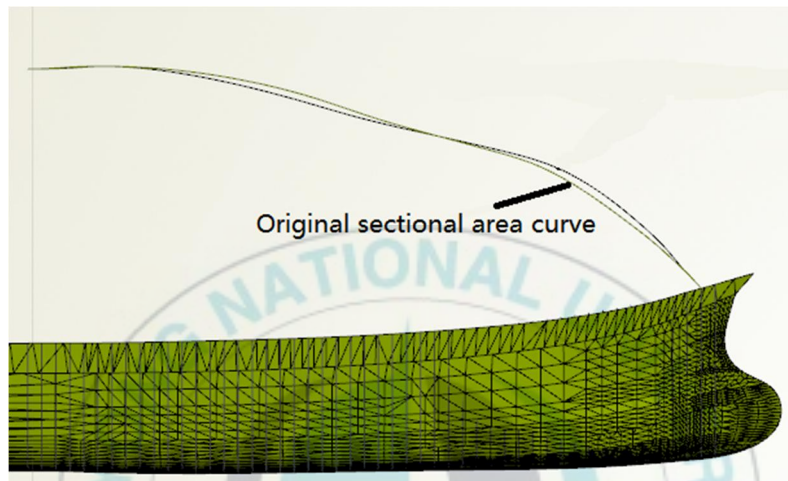


Fig.4.8 Bow part LCB moving forward by 0.4%

Fig.4.9 shows the bow part of catamaran demi-hull modified under the constraints of LCB moving backward by 0.4%, the design variables will be  $\Delta\text{LCB}=-0.4$ .

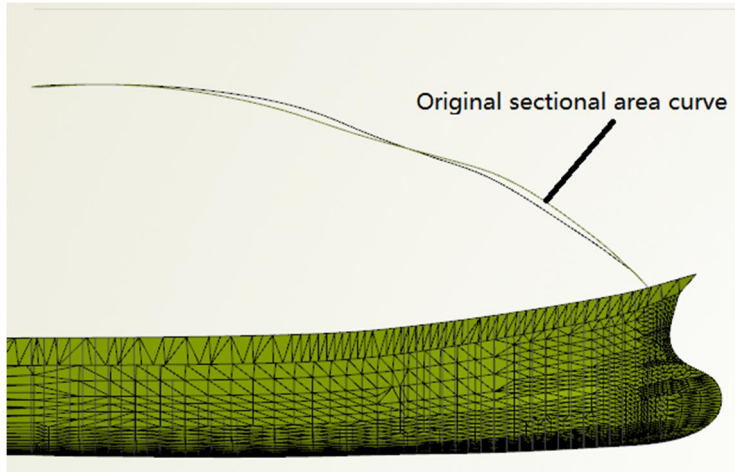


Fig.4.9 Bow part LCB moving backward by 0.4%

## 4.5 Optimization Results and Analysis

The whole flow chart of this demi-hull optimization loop is shown in Fig.4.10.

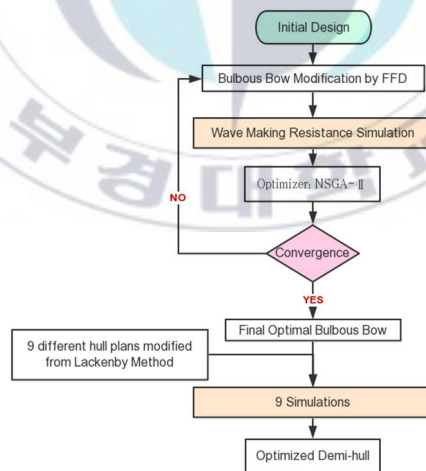


Fig.4.10 Demi-hull optimization loop flow chart in this study

In this study, wave making resistance of catamaran in calm water was selected to be the object function in the whole optimization process. Catamaran demi-hulls' wave making resistance performance in calm water was optimized first and then the distance between demi-hulls was optimized. The optimization process is listed below:

Firstly, Free-Form Deformation (FFD) method was employed to modify the bulbous bow shape with the design variables: length, breadth, and angle(between bulbous bow and baseline).

Coupling CAD and CFD solver(CAESES and StarCCM+), 200 simulations were carried and compared to get the optimal bulbous bow No.1

Then optimization method: Non-dominated Sorting Genetic Algorithm (NSGA)-II was employed to get optimal bulbous bow No.2.

Comparing optimal bulbous bow No.1 and No.2, get the final bulbous bow.

Then the bow part between bulbous bow and mid-ship was modified by Lackenby method (shifting the section curve) design variable: Longitudinal Centre of Buoyancy(LCB).

9 different plans from Lackenby method were computed and the optimized demi-hull form was obtained.

#### 4.5.1 Bulbous Bow Optimization Results and Analysis

The wave making resistance was simulated in StarCCM+ and feed back to CAESES so the optimal bulbous bow can be found easily. Two different ways of the bulbous bow optimization were carried in this study at  $Fn=0.73$ .

The first way is normally implementing 200 simulations of 200 different hull forms. The bulbous bow of the demi-hull is generated from the FFD method with 3 design variables: length, breadth, and angle.

Fig.4.11 is the results of wave making resistance of 200 different bulbous bow plans. They are from 200 simulations carried by StarCCM+. The redpoint represent the optimal solution NO.1.

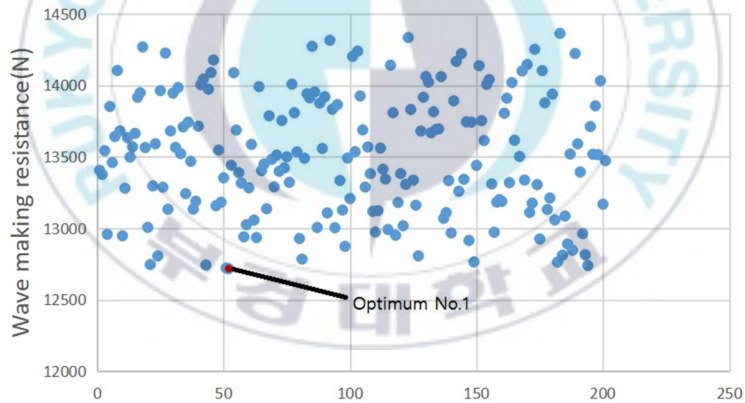


Fig.4.11 Wave making resistance of 200 different bulbous bow plans

Fig.4.12 is the results of wave making resistance of 5 generations of different bulbous bow plans total 135. They are from 135 simulations carried by StarCCM+. The noted point represents the optimal solution NO.2.

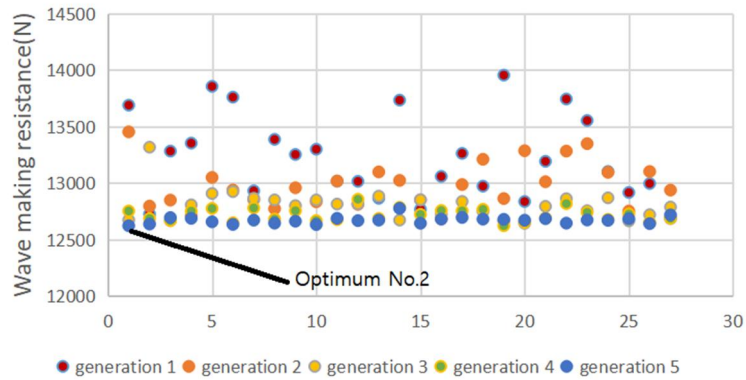


Fig.4.12 Wave making resistance of 5 generations of different bulbous bow plans

Table 4.1 is the comparison of the two optimal bulbous bows from two different optimization process. The  $R_w$  of No.2 Bulbous bow plan from NSGA-II method is smaller than No.2 (Differents:0.7% ). The No.2 bulbous bow will be selected for the next optimization.

Table 4.1 Comparison of optimal bulbous bows from two optimization process

Items	optimum No.1	optimum No.2
length	1.02	1.018
breadth	1.3	1.14
angle	3°	2.64°
$R_w$ (N)	25436	25246
$C_w$ (10-3)	5.238	5.201
$R_w$ reduction(%)	4.6	5.3

Fig.4.13~Fig.4.15 show the evolution trend of the three parameters: length, breadth, and angle. It can be seen that the length value converges to 1.018, the breadth value converge to 1.14 and the angle converges to 2.64°.

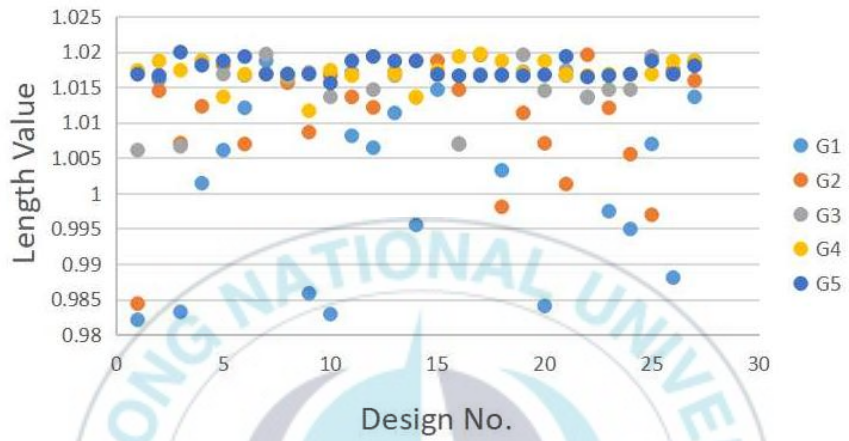


Fig.4.13 Length evolution trend of 5 generations of different bulbous bow plans

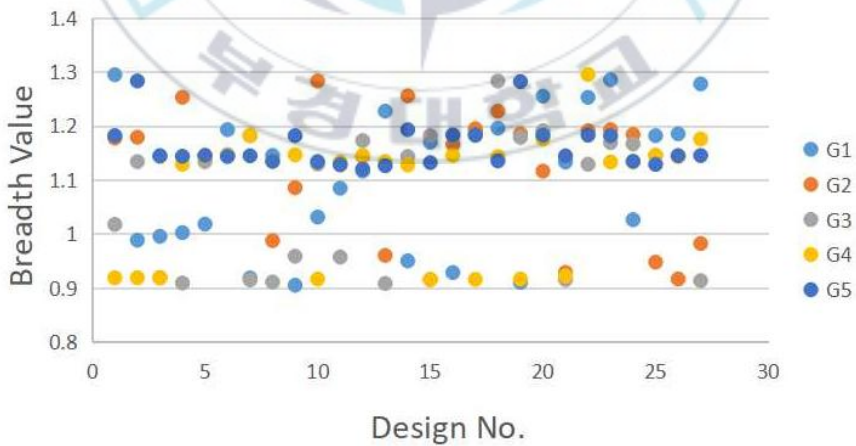


Fig.4.14 Breadth evolution trend of 5 generations of different bulbous bow plans

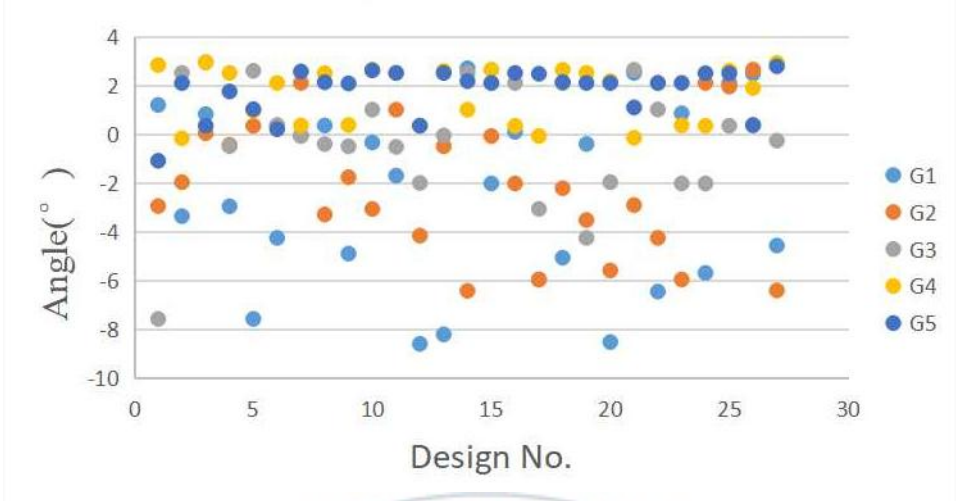


Fig.4.15 Angle evolution trend of 5 generations of different bulbous bow plans

Fig.4.16 shows the is the profile of the three different bulbous bows. Optimum No.1 and optimum No.2 has no big difference, and both bulbous bows has a big difference with the original bulbous bow. Results show that optimization is necessary.

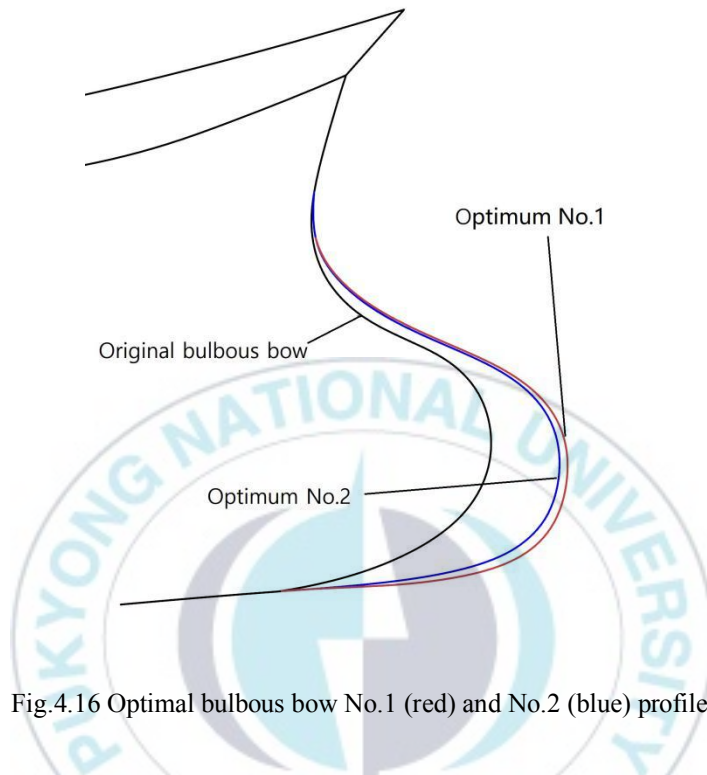


Fig.4.16 Optimal bulbous bow No.1 (red) and No.2 (blue) profile

#### 4.5.2 Bow Part Optimization Results and Analysis

The bow part between bulbous bow and mid-ship was modified by Lackenby method (shifting the section curve) design variable: change of Longitudinal Centre of Buoyancy( $\Delta LCB$ ). 9 different plans from Lackenby method were computed and the optimized demi-hull form was obtained.

Fig. 4.17 is the simulating results of the 9 different plans from Lackenby method. The result shows the wave making resistance reduced for about 1 percent

when the longitudinal center of buoyancy moves backward for 0.3 percent by Lackenby method.

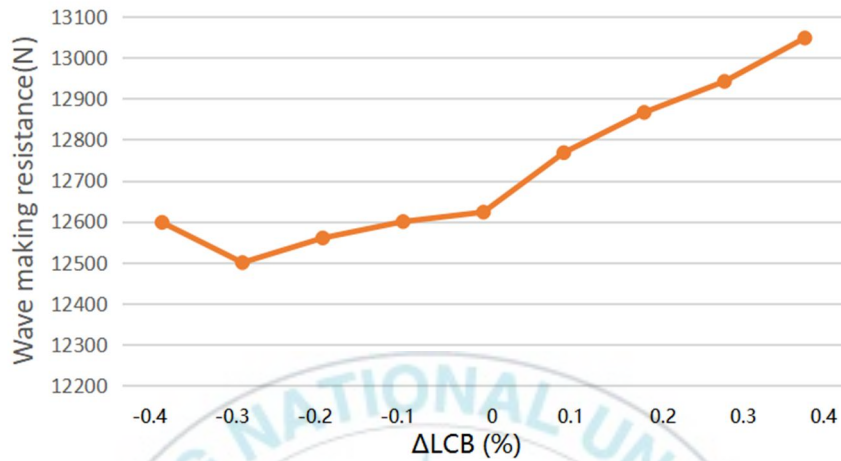
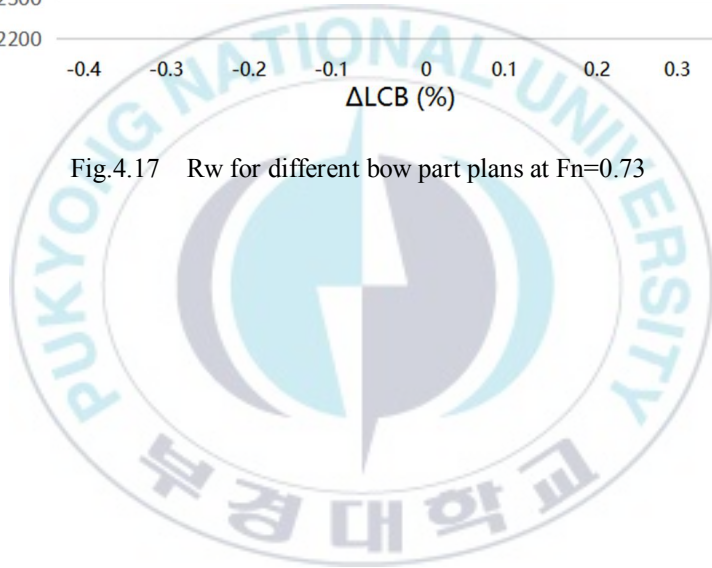


Fig.4.17  $R_w$  for different bow part plans at  $Fn=0.73$



## V Distance Between Demi-hulls Optimization

Since the optimal demi-hull is obtained as it was introduced in chapter IV, the distance between catamaran demi-hulls will be optimized in this chapter.

### 5.1 Theoretical Background of Interference of Catamaran Demi-hulls

The catamaran resistance problem has been discussed in the scientific forum because its resistance components are more complex than mono-hulls. This is due to the complexity of the interaction and the interference of the catamaran's wave-damping components. In the past, there have been several studies on catamaran resistance, including early experiments. The interference phenomena are generated by variation of velocity field around demi-hulls, change of form factor value and superimposition of wave patterns. The general trend in all cases is that as the hull separation and stagger are increased, the resistance decreases.

The resistance and interference factors are significantly affected by the symmetrical hull compared to the asymmetrical one. Usually, the interference between the demi-hulls of a symmetric catamaran is negative to the total wave making resistance. It was considered that the distance between the demi-hulls has a positive correlation with the total wave making resistance. The distance between the demi-hulls more bigger, the negative interference of the two demi-hulls is weaker. But it also related to the Froude number of the catamaran.

According to Millward (1992), the effect of hull separation on catamaran resistance can be summarized in Fig.5.1.  $S$  represents the separation of the two demi-hulls.  $L$  represents the length of the demi-hull.

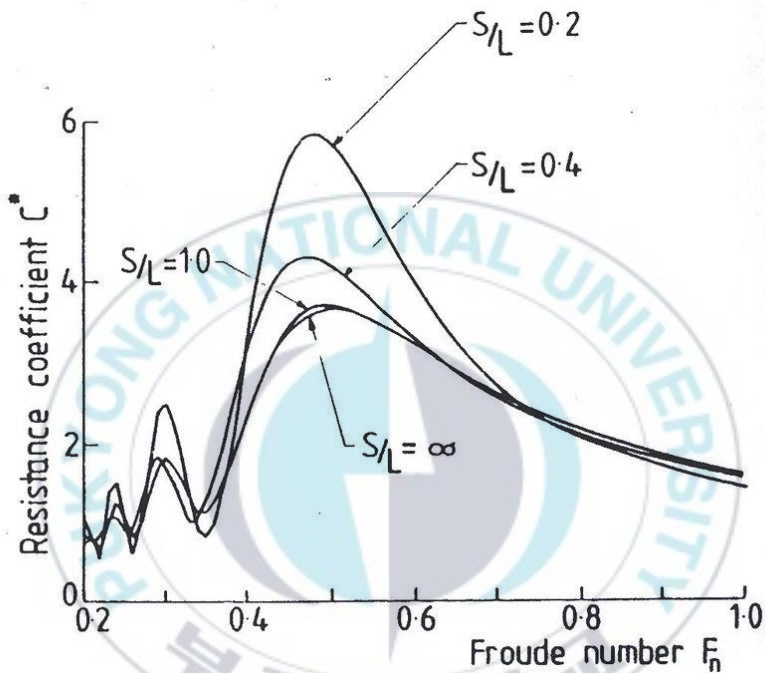


Fig.5.1 The effect of demi-hull separation on catamaran resistance at different  $F_n$  [Millward (1992)]

In Fig.5.1, the effect on resistance coefficient is separated into three parts. The effect of the distance has no rules to follow when the  $F_n$  ranges from around 0.2 to 0.4. In the  $F_n$  range between 0.4 and 0.7, there is a trend that the distance between the demi-hulls has a positive correlation with the total wave making resistance. The

distance between the demi-hulls more bigger, the negative interference of the two demi-hulls is weaker. When the  $F_n$  of the catamaran is beyond 0.7, the lines of resistance coefficient began to cross that means the effect of the distance also has no rules to follow. But we do know the potential optimal distance maybe exist.

In this case, with the design speed of the catamaran,  $F_n$  is 0.73. The calculation of the wave making resistance of the different plans from the different distance between demi-hulls will be carried and try to find out the effect of the demi-hull separation.

## **5.2 Distance Between Demi-hulls Optimization**

The distance between demi-hulls optimization is not very complicated progress. The optimum was considered to be able to be found by several simulations because the effect of the distance has a certain trend according to section 5.1.

19 different plans for the separation of the two demi-hulls was generated and simulated in this section. The results were shown in Fig.5.2. The wave making resistance of the catamaran has the smallest value when the  $S/L$  value is 0.42.  $S$  means the separation or distance between the two demi-hulls and  $L$  means the length of the catamaran.

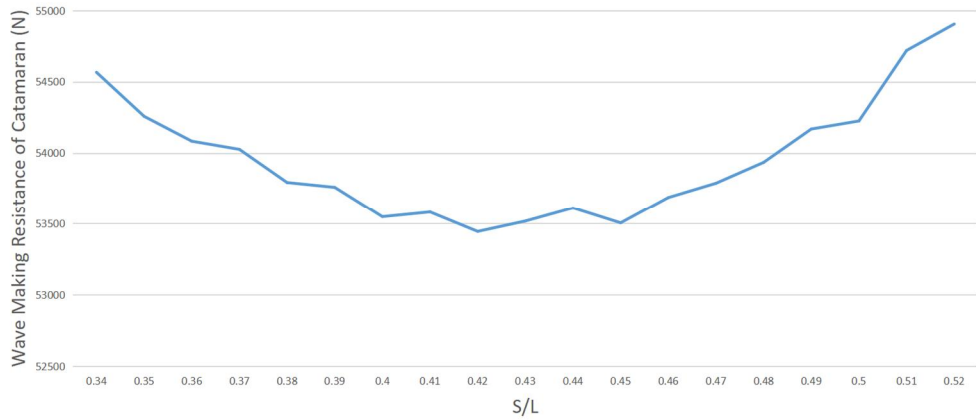


Fig.5.2 The  $R_w$  of catamaran resistance at different separation plans

According to section 5.1, The  $R_w$  of the catamaran is usually a little bigger than the twice of  $R_w$  of demi-hull. The  $R_w$  of the catamaran was compared to the  $R_w$  of demi-hull in Fig.5.3. The results difference is around 1.069 to 1.093, it means the simulating results are reasonable.

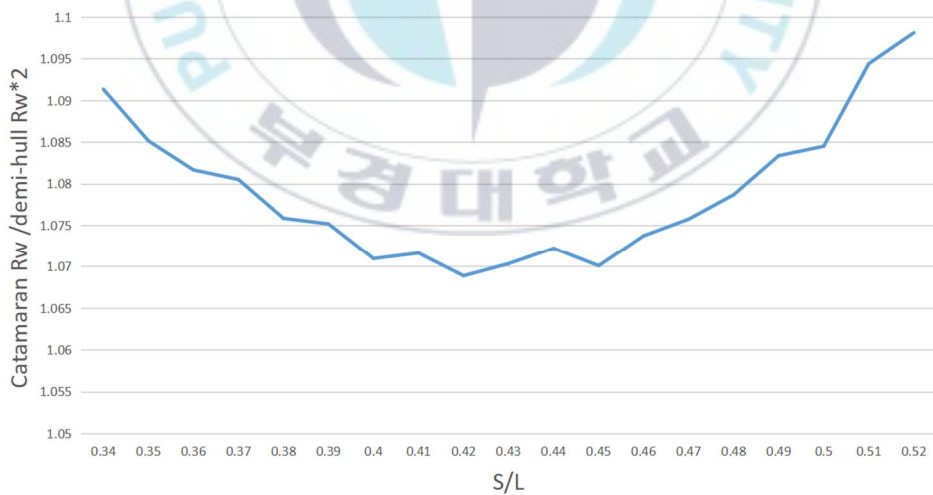


Fig.5.3 The  $R_w$  difference of catamaran and two demi-hulls at different separation plans

The results show the distance between demi-hulls of a catamaran does has optimal value in this case. It is because the catamaran has high design speed ( $F_n=0.73$ ).



# VI Conclusion and Future Work

## 6.1 Conclusion

By coupling the software CAESES and StarCCM+, the wave making resistance of a high-speed catamaran was optimized in this study. R<sub>w</sub> simulation was carried in RANS method but the fluid model was set to be inviscid. The computing time reduced for 50 percent and comparing to the viscous flow and the simulating results has no more than 1 percent difference.

The bulbous bow of the demi-hull was optimized by genetic algorithm. The design variables were generated by Free-Form deformation method in the bulbous bow length, breadth, and angle. The bow part between bulbous bow and mid-ship was optimized by simulating 9 different plans modified by Lackenby method keeping the displacement of the demi-hull constant. The design variable is the change of the longitudinal center of buoyancy. The distance between two demi-hulls was optimized by simulating 19 different separation plans.

The wave making resistance of the optimal demi-hull has reduced for 6.2 percent comparing to the original demi-hull. The total resistance of the catamaran has the optimal performance when the distance of two demi-hulls is 8.4m (S/L=0.42). Results show that this optimization loop is feasible and efficient.

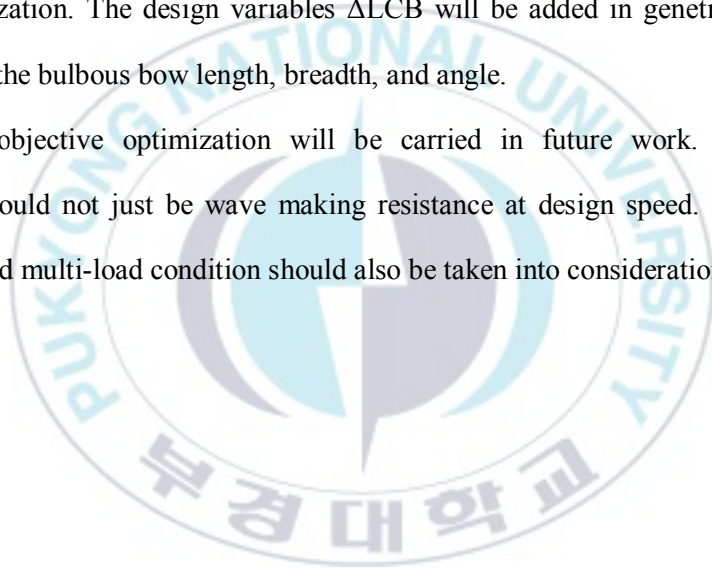
There are still some disadvantages in this optimization loop. FFD method implemented at the bulbous bow can result in the hull form not being smooth sometimes.

The bulbous bow will affect the flow so the optimal bulbous bow to the original hull form does not mean the optimal bulbous bow to the optimal bow part plan modified by Lackenby method. And the simulation results was not been compared to experimental results.

## 6.2 Future Work

The future work will focus on combining the bulbous bow optimization to bow part optimization. The design variables  $\Delta LCB$  will be added in genetic algorithm along with the bulbous bow length, breadth, and angle.

Multi-objective optimization will be carried in future work. The object function should not just be wave making resistance at design speed. Multi-speed situation and multi-load condition should also be taken into consideration.



## References

- A. Coppedé, G. Vernengo & D. Villa, A combined approach based on Subdivision Surface and Free Form Deformation for smart ship hull form design and variation, *Ships and Offshore Structures*, 2018, VOL. 13, NO. 7, 769–778.
- Chrismianto D, Kim DJ, Parametric bulbous bow design using the cubic Bezier curve and curve-plane intersection method for the minimization of ship resistance in CFD, *Journal of Marine Science and Technology*, Volume19, Issue4(2014) pp:479-492.
- F. X. Huang, L. L. Wang and C. Yang, A new improved artificial bee colony algorithm for ship hull form optimization, *Engineering Optimization*(2016), Vol. 48, No. 4, 672–686.
- J.Y. He, C.L. Zhang, Y. Zhu, L. Zou, W. Li, F. Noblesse, Interference effects on the Kelvin wake of a catamaran represented via a hull-surface distribution of sources *European Journal of Mechanics B/Fluids* (2016), Vol. 56, 1-12.
- J. W. Wu, X. Y. Liu, M. Zhao, D. C. Wan, Neumann-Michell theory-based multi-objective optimization of hull form for a naval surface combatant, *Applied Ocean Research*, 63 (2017) 129–141.
- K.A.P. Utama, A. Jamaluddin, W.D. Aryawan, Experimental Investigation Into The Drag Interference of Symmetrical and Asymmetrical Staggered and Unstaggered Catamarans, *Technology to the Wind* (2012), Vol. 7, No. 1, 47-58.
- Luo, WL, Lan, LQ. Design Optimization of the Lines of the Bulbous Bow of a Hull Based on Parametric Modeling and Computational Fluid Dynamics Calculation. *Math. Comput. Appl.* 2017, 22, 4.
- M. Iqbal & Samuel, Traditional Catamaran Hull Form Configurations that Reduce Total Resistance, *International Journal of Technology* (2017) 1: 989-997.
- Molland, A.F., Wellicome, J.F., Couser, P., 1996. Resistance Experiments on a Systematic Series of High-Speed Displacement Catamaran Forms: Variations of Length-Displacement Ratio and Breadth-Draught Ratio. *Transaction RINA*, Volume 138A, pp. 59–71.
- Molland, A.F., Wilson, P.A., Taunton, D.J., Chandrababha, S., Ghani, P.A., 2004. Resistance and Wash Wave Measurements on a Series of High-Speed Displacement

- Monohull and Catamaran Forms in Shallow Water. *The International Journal of Maritime Engineering*, Volume 146(a2), pp. 19–38.
- Pien, P.C., 1976. Catamaran Hull-Form Design. *In: International Seminar on Wave Resistance*, Society of Naval Architects of Japan (SNAJ), pp. 14–25.
- Sederberg TW, Parry SR, Free-form deformation of solid geometric models, *ACM SIGGRAPH Comput Graph*, Volume20,Issue4(1986)pp:151–160.
- S. L. Zhang, B. J. Zhang, T. Tezdogan, L.P. Xu and Y. Y. Lai, Computational fluid dynamics-based hull form optimization using approximation method, *Engineering Applications of Computational Fluid Mechanics*, 2018, VOL. 12, NO. 1, 74–88.
- S. H. Han, Y. S. Lee, Y. B. Choi, Hydrodynamic hull form optimization using parametric models, *J Mar Sci Technol* (2012) 17:1–17.
- Samuel, Iqbal, M., Utama, I.K.A.P., 2015. An Investigation into the Resistance Components of Converting a Traditional Monohull Fishing Vessel into Catamaran Form. *International Journal of Technology*, Volume 6(3), pp. 432–441.
- Seif, M.S., Amini, E., 2004. Performance Comparison Between Planing Monohull and Catamaran at High Froude Numbers. *Iranian Journal of Science & Technology*, Volume 28(B4), pp. 435–441.
- Setyawan, D., Utama, I.K.A.P., Sugiarto, A., Jamaluddin, A., 2010. Development of Catamaran Fishing Vessel. *The Journal for Technology and Science*, Volume 21(4), pp. 2–9.
- T. Tezdogana,, Zhang Shenglongb, Yigit Kemal Demirela, Wendi Liua, Xu Lepingb, Lai Yuyangc, Rafet Emek Kurta, Eko Budi Djatmikod, Atilla Incecika, An investigation into fishing boat optimisation using a hybrid algorithm, *Ocean Engineering*, 167(2018) 204-220.
- K.V. Kostas, A.I. Ginnis, C.G. Politis, P.D. Kaklis, Ship-hull shape optimization with a T-spline based BEM–isogeometric solver, *Comput. Methods Appl. Mech. Engrg.* 284 (2015) 611–622.
- X. D Cheng, B. W. Feng , Z. Y. Liu , H. C. Chang, Hull surface modification for ship resistance performance optimization based on Delaunay triangulation, *Ocean Engineering*, 153(2018) 333-344.

CAESES 및 StarCCM+ 를 사용하여 쌍동선 선수부분 빠른 최적화 루프 개발

장영홍

부경대학교 대학원 마린융합디자인협동과정

### 국문요약

최근 개인용 전산기의 발전된 계산 속도로 인해 선형 최적화에 CFD를 적용하는 연구가 많이 이루어지고 있다. 그리고 CAD와 CFD, 그리고 최적화 과정까지 하나의 통합프로그램으로 구현하여 효율성을 높인 프로그램들도 발표되고 있다. CASES도 이러한 프로그램으로, 전형적인 CAD-CFD integration platform 이다.

본 논문에서는 CASES를 이용하여 쌍동선의 선형을 최적화 하고자 하였다. 선형을 변환시키는 방법으로는 Lackenby method 와 Free-Form Deformation method를 사용하였다. 쌍동선 demi-hull의 선수부분 형상을 변화시키기 위해 배수량을 변화시키지 않고 LCB를 변화시키는 Lackenby method를 사용하였고, bulbous bow의 형상을 바꾸기 위해 Free-Form Deformation method를 적용하였으며, 길이, Bulb girth 길이, Bulb와 기선과의 사이 각도 등을 파라미터로 선택하였다. CFD-Solver로는 StarCCM+을 사용하였으며, 최적화 기법으로는 Non-dominated Sorting Genetic Algorithm (NSGA)-II를 적용하였다. 얻어진 최적 demi-hull 선형을 이용하여 쌍동선의 두 개의 demi-hull 간격도 최적화 하였다.

**키워드:** 쌍동선, Free-Form Deformation, Lackenby, 조파저항, 최적화

## Acknowledgment

Studying abroad can be a big challenge for most of the candidates. Fortunately, I had the most amazing 2 years in Korea that I would always cherish. I will never go so far without all the help and care I have received here.

First of all, I would like to deepest thank to my adviser Professor Dong-Joon Kim. I would thank him for teaching me with a passion so that I can feel the charm of ship engineering. I would thank him for guiding me with patience so that I can bring out all my puzzles without feeling stupid. I would thank him for treating me with kindness letting me feel home in the lab. I would thank him for always being so supportive and fixing all the problems I had met in school. I will never go so far without Professor Kim's help.

I would also thank the other Professors in my apartment for giving such great lectures and advice. Thank Prof. Joung Hyung Cho, Prof. Jung Min Sohn for the valuable advice for the thesis. I would like to express my special thank to Professor Sang-Mook Shin, for the great support on meshing strategy and CFD theory. Thank my seniors Yeon-Hee Song, Seung-Woo Shin and lab members Aldias Bahatmaka, Samuel, May Thu Zaw and Thandar Aung for supporting and treating me like families.

Thank the Brain of Korea project for the scholarship fund and the teachers. Because of them, I can concentrate on my study free of worrying about financial difficulties.

Finally, I would like to thank my beautiful girlfriend XuGuoDing for always being so thoughtful and supportive. Also, thank my families and my friends in China for the support and talking to me when I feel bored.

## Appendix

Appendix A: Data of Bulbous Bow Optimization Using NSGA-II

Appendix B: Data of Bulbous Bow Optimization of 200 Simulations



Appendix A: Data of Bulbous Bow Optimization Using NSGA-II

Design No.	angle	breadth	length	Rw (N)
Nsga2_10_des0000	1.194	1.29469	0.982097	13689.9
Nsga2_10_des0001	-3.36301	0.988356	1.01611	12932.6
Nsga2_10_des0002	0.817716	0.995412	0.983228	13734.6
Nsga2_10_des0003	-2.95889	1.00213	1.00141	13283.8
Nsga2_10_des0004	-7.57762	1.01807	1.00608	13354.3
Nsga2_10_des0005	-4.25585	1.19296	1.01206	13016.1
Nsga2_10_des0006	-0.0566262	0.91828	1.0187	12768.6
Nsga2_10_des0007	0.354818	1.14517	1.01683	12727.1
Nsga2_10_des0008	-4.89856	0.904883	0.985848	13856.3
Nsga2_10_des0009	-0.343008	1.03104	0.982904	13761
Nsga2_10_des0010	-1.7035	1.08445	1.00811	13017.9
Nsga2_10_des0011	-8.59973	1.11627	1.00642	13387.7
Nsga2_10_des0012	-8.21135	1.22719	1.01134	13253.8
Nsga2_10_des0013	2.6986	0.949934	0.995513	13300.6
Nsga2_10_des0014	-2.02449	1.16952	1.01464	12866.2
Nsga2_10_des0015	0.0907759	0.928266	1.00692	13059.7
Nsga2_10_des0016	-5.95875	1.19082	1.01956	12973.5
Nsga2_10_des0017	-5.06757	1.19552	1.00323	13263.6
Nsga2_10_des0018	-0.406546	0.910108	1.01716	12837.8
Nsga2_10_des0019	-8.52447	1.25504	0.984056	13955.7
Nsga2_10_des0020	2.50707	1.13307	1.01662	12687.2
Nsga2_10_des0021	-6.45663	1.25281	1.01353	13103.3
Nsga2_10_des0022	0.850126	1.28536	0.997449	13193.4
Nsga2_10_des0023	-5.69178	1.02615	0.994936	13554.3
Nsga2_10_des0024	2.09673	1.18181	1.00695	12917.5
Nsga2_10_des0025	2.47979	1.18525	0.988071	13454
Nsga2_10_des0026	-4.56988	1.27769	1.01361	12996.8
Nsga2_10_des0027	-2.95102	1.17741	0.984387	13744.6

Design No.	angle	breadth	length	Rw (N)
Nsga2_10_des0028	-1.97176	1.1789	1.01448	12849.9
Nsga2_10_des0029	0.0380407	0.918891	1.00707	13050.7
Nsga2_10_des0030	-0.441886	1.25299	1.01228	12835.2
Nsga2_10_des0031	0.340169	1.14499	1.01808	12710.4
Nsga2_10_des0032	0.354818	1.14507	1.00694	12959.2
Nsga2_10_des0033	2.09673	1.18191	1.01681	12685.4
Nsga2_10_des0034	-3.29709	0.987526	1.01561	12939.8
Nsga2_10_des0035	-1.76942	1.08544	1.00862	13024.4
Nsga2_10_des0036	-3.06986	1.28308	1.01662	12853.5
Nsga2_10_des0037	1.00119	1.12768	1.01361	12797.2
Nsga2_10_des0038	-4.1621	1.14296	1.01212	13018.9
Nsga2_10_des0039	-0.500298	0.960108	1.01706	12812.5
Nsga2_10_des0040	-6.42586	1.25554	1.01354	13099.4
Nsga2_10_des0041	-0.081529	0.915534	1.01869	12774.2
Nsga2_10_des0042	-2.02449	1.16581	1.01464	12852.6
Nsga2_10_des0043	-5.96461	1.19453	1.01956	12987.8
Nsga2_10_des0044	-2.2195	1.22724	0.998072	13283.7
Nsga2_10_des0045	-3.52378	1.18529	1.01134	13012.7
Nsga2_10_des0046	-5.58796	1.11612	1.00705	13211.3
Nsga2_10_des0047	-2.90927	0.928412	1.00129	13318.4
Nsga2_10_des0048	-4.25585	1.19082	1.01956	12863.9
Nsga2_10_des0049	-5.95875	1.19296	1.01206	13103.2
Nsga2_10_des0050	2.09673	1.18415	1.00551	12938.6
Nsga2_10_des0051	1.94859	0.94759	0.996945	13287
Nsga2_10_des0052	2.64038	0.916358	1.01737	12753.3
Nsga2_10_des0053	-6.40993	0.982106	1.01591	13095.6
Nsga2_10_des0054	-7.57762	1.01738	1.00608	13349.5
Nsga2_10_des0055	2.50707	1.13376	1.01662	12674.6
Nsga2_10_des0056	2.9436	1.14313	1.00662	12908.7
Nsga2_10_des0057	-0.493156	0.908905	1.0187	12808.2

Design No.	angle	breadth	length	Rw (N)
Nsga2_10_des0058	2.59313	1.13376	1.01683	12665.7
Nsga2_10_des0059	0.362509	1.14673	1.01663	12724.1
Nsga2_10_des0060	-0.0784161	0.914795	1.01966	12750.3
Nsga2_10_des0061	-0.409659	0.910846	1.01619	12851.9
Nsga2_10_des0062	-0.500298	0.958546	1.01706	12815.2
Nsga2_10_des0063	1.00119	1.12924	1.01361	12801.5
Nsga2_10_des0064	-0.523735	0.956983	1.01706	12817.4
Nsga2_10_des0065	-2.00105	1.17265	1.01464	12852.3
Nsga2_10_des0066	-0.0566262	0.908124	1.01662	12838.4
Nsga2_10_des0067	2.50707	1.14323	1.0187	12644.6
Nsga2_10_des0068	2.09673	1.18191	1.01673	12668.8
Nsga2_10_des0069	2.09673	1.18181	1.00702	12925.2
Nsga2_10_des0070	-3.06693	1.18191	1.0168	12866.5
Nsga2_10_des0071	2.0938	1.28308	1.01661	12673.4
Nsga2_10_des0074	-4.25585	1.17871	1.01956	12885.1
Nsga2_10_des0075	-1.97176	1.19101	1.01448	12853.2
Nsga2_10_des0076	2.64038	0.915186	1.01736	12756.8
Nsga2_10_des0077	1.00705	1.12885	1.01362	12795
Nsga2_10_des0078	-2.02449	1.16894	1.01464	12870.3
Nsga2_10_des0079	-2.02449	1.1664	1.01464	12862.8
Nsga2_10_des0080	0.340169	1.14517	1.01933	12666.2
Nsga2_10_des0081	0.354818	1.14499	1.01683	12721.2
Nsga2_10_des0082	-0.269032	0.913239	1.01871	12789.1
Nsga2_10_des0083	2.82788	0.918653	1.01735	12754
Nsga2_10_des0084	-0.172351	0.918671	1.01868	12776.5
Nsga2_10_des0085	2.9436	0.918262	1.01737	12752.9
Nsga2_10_des0086	2.50561	1.12882	1.0187	12649.6
Nsga2_10_des0087	0.960174	1.14325	1.01362	12786.1
Nsga2_10_des0090	2.09691	1.14517	1.01683	12677.1
Nsga2_10_des0091	0.354635	1.18269	1.01681	12723.7

Design No.	angle	breadth	length	Rw (N)
Nsga2_10_des0092	2.49535	1.13423	1.01662	12687.8
Nsga2_10_des0093	0.374228	1.14626	1.01163	12857.4
Nsga2_10_des0094	2.64038	0.91626	1.01737	12755.2
Nsga2_10_des0095	2.50707	1.13317	1.01662	12687.4
Nsga2_10_des0096	0.343099	1.14517	1.01933	12668.7
Nsga2_10_des0097	2.5902	1.13376	1.01683	12668.5
Nsga2_10_des0098	0.999725	1.12768	1.01361	12781.2
Nsga2_10_des0099	2.64184	0.915186	1.01736	12756.5
Nsga2_10_des0102	0.340169	1.14517	1.01931	12682.5
Nsga2_10_des0103	-0.0784161	0.915576	1.01968	12758
Nsga2_10_des0104	2.64038	1.14323	1.0187	12623.8
Nsga2_10_des0105	2.50707	0.916358	1.01706	12768.5
Nsga2_10_des0106	2.16997	1.17566	1.01868	12652.8
Nsga2_10_des0107	-0.154772	0.921784	1.01673	12819.2
Nsga2_10_des0108	2.09087	1.29519	1.01661	12680
Nsga2_10_des0109	0.357748	1.13306	1.01683	12727.1
Nsga2_10_des0110	0.343099	1.13376	1.01683	12741.9
Nsga2_10_des0111	2.60485	1.14499	1.01683	12692.1
Nsga2_10_des0112	1.89036	1.14323	1.0187	12658.3
Nsga2_10_des0113	2.91998	1.17566	1.01868	12638.2
Nsga2_10_des0114	-1.09375	1.18191	1.01681	12777.2
Nsga2_10_des0115	2.09087	1.28308	1.01661	12668.8
Nsga2_10_des0116	0.348959	1.14478	1.01993	12655
Nsga2_10_des0117	1.74827	1.14362	1.01807	12673.3
Nsga2_10_des0118	2.781	1.14518	1.0187	12635.2
Nsga2_10_des0119	0.199542	1.14322	1.01931	12688.6
Nsga2_10_des0120	2.56567	1.14458	1.01683	12688.7
Nsga2_10_des0121	2.12438	1.13434	1.01683	12695.6
Nsga2_10_des0122	2.07768	1.18191	1.01683	12663.6
Nsga2_10_des0123	2.61218	1.13376	1.01556	12689.1

Design No.	angle	breadth	length	Rw (N)
Nsga2_10_des0124	2.50561	1.12843	1.0187	12646.5
Nsga2_10_des0125	0.343099	1.12017	1.01932	12673
Nsga2_10_des0126	2.50707	1.12604	1.01868	12633.8
Nsga2_10_des0127	2.16997	1.19285	1.0187	12645.3
Nsga2_10_des0128	2.09691	1.1319	1.01678	12696.6
Nsga2_10_des0129	2.50689	1.18318	1.01659	12681.8
Nsga2_10_des0130	2.47192	1.18307	1.01662	12679.9
Nsga2_10_des0131	2.13188	1.13506	1.01673	12681.9
Nsga2_10_des0132	2.09673	1.2819	1.01661	12672.4
Nsga2_10_des0133	2.09087	1.18269	1.01673	12685.8
Nsga2_10_des0134	1.09311	1.14439	1.01933	12646.4
Nsga2_10_des0135	2.09673	1.18269	1.01642	12674.4
Nsga2_10_des0136	2.09673	1.1819	1.01662	12670.9
Nsga2_10_des0137	2.49535	1.13424	1.01681	12685.7
Nsga2_10_des0138	2.48803	1.12858	1.0187	12642.3
Nsga2_10_des0139	0.372396	1.14445	1.01683	12719.5

Appendix B: Data of Bulbous Bow Optimization of 200 Simulations

Design No.	length	breadth	angle	Rw (N)
design_001	0.98	0.8	-6	14268.8
design_002	0.98	1	0	14022
design_003	0.98	0.9	-6	14221.7
design_004	0.98	1	-6	14202.2
design_005	0.98	1	-9	14315.2
design_006	0.98	1	3	13972.9
design_007	0.98	1	-3	14102.9
design_008	0.98	0.9	3	13984.7
design_009	0.98	0.9	0	14031.3
design_010	0.98	0.8	-3	14177.1
design_011	0.98	0.9	-3	14137.2
design_012	0.98	0.9	-9	14333.9
design_013	0.98	0.8	0	14089.1
design_014	0.98	0.8	3	14006.4
design_015	0.98	0.8	-9	14363.1
design_016	0.98	1.1	0	13990.8
design_017	0.98	1.1	-3	14087.9
design_018	0.98	1.1	-6	14166.7
design_019	0.98	1.2	3	13891.6
design_020	0.98	1.2	0	13953.6
design_021	0.98	1.2	-9	14252.1
design_022	0.98	1.2	-6	14141
design_023	0.98	1.1	3	13941.2
design_024	0.98	1.1	-9	14272.7
design_025	0.98	1.2	-3	14060.8
design_026	0.98	1.3	0	13945.4
design_027	0.98	1.3	3	13877.9

design_028	0.98	1.3	-3	14040.2
Design No.	length	breadth	angle	Rw (N)
design_029	0.98	1.3	-6	14145.6
design_030	0.98	1.3	-9	14239.1
design_031	0.98	1.4	3	13865.3
design_032	0.98	1.4	-6	14100.3
design_033	0.98	1.4	-9	14222.3
design_034	0.98	1.4	0	13925.6
design_035	0.98	1.5	3	13832.4
design_036	0.98	1.5	0	13920.3
design_037	0.98	1.5	-6	14103.5
design_038	0.98	1.5	-3	14004.7
design_039	0.98	1.4	-3	14019.6
design_040	0.99	0.8	3	13687.9
design_041	0.98	1.5	-9	14225.7
design_042	0.99	0.8	-3	13856.7
design_043	0.99	0.8	0	13753
design_044	0.99	0.8	-6	13963
design_045	0.99	0.9	3	13614.3
design_046	0.99	0.8	-9	14061.8
design_047	0.99	0.9	-3	13831.2
design_048	0.99	0.9	0	13709.3
design_049	0.99	0.9	-6	13916.8
design_050	0.99	0.9	-9	14043.1
design_051	0.99	1	3	13586.7
design_052	0.99	1	0	13681.1
design_053	0.99	1	-9	14007.7
design_054	0.99	1	-3	13753.8
design_055	0.99	1	-6	13875.8
design_056	0.99	1.1	3	13558.3
design_057	0.99	1.1	0	13634.4

design_058	0.99	1.1	-6	13852.1
Design No.	length	breadth	angle	Rw (N)
design_059	0.99	1.1	-3	13744.6
design_060	0.99	1.1	-9	13948.3
design_061	0.99	1.2	-6	13815.1
design_062	0.99	1.2	-3	13742.9
design_063	0.99	1.2	0	13591
design_064	0.99	1.2	-9	13916.4
design_065	0.99	1.2	3	13512.2
design_066	0.99	1.3	3	13502.9
design_067	0.99	1.3	0	13590.8
design_068	0.99	1.3	-3	13713.9
design_069	0.99	1.3	-6	13804.9
design_070	0.99	1.3	-9	13938.4
design_071	0.99	1.4	0	13564.8
design_072	0.99	1.4	3	13500
design_073	0.99	1.4	-6	13807.9
design_074	0.99	1.4	-9	13912.5
design_075	0.99	1.4	-3	13668.7
design_076	0.99	1.5	-3	13681.1
design_077	0.99	1.5	0	13569.5
design_078	0.99	1.5	3	13482.3
design_079	0.99	1.5	-9	13909.9
design_080	1	0.8	3	13377.6
design_081	1	0.8	0	13440
design_082	0.99	1.5	-6	13786.6
design_083	1	0.8	-3	13568.8
design_084	1	0.8	-6	13680.1
design_085	1	0.9	3	13344.5
design_086	1	0.8	-9	13808.8
design_087	1	0.9	0	13413.7

design_088	1	0.9	-3	13497.8
Design No.	length	breadth	angle	Rw (N)
design_089	1	0.9	-6	13615.6
design_090	1	0.9	-9	13742.7
design_091	1	1	3	13287.2
design_092	1	1	0	13336.9
design_093	1	1	-3	13472.9
design_094	1	1	-6	13566
design_095	1	1	-9	13711.8
design_096	1	1.1	3	13212
design_097	1	1.1	-3	13440.8
design_098	1	1.1	0	13334.4
design_099	1	1.1	-6	13543
design_100	1	1.1	-9	13695.4
design_101	1	1.2	-3	13404
design_102	1	1.2	0	13316.1
design_103	1	1.2	3	13190
design_104	1	1.2	-6	13518.2
design_105	1	1.2	-9	13664.1
design_106	1	1.3	3	13183
design_107	1	1.3	-3	13398.8
design_108	1	1.3	0	13288.5
design_109	1	1.3	-6	13534.2
design_110	1	1.3	-9	13641.6
design_111	1	1.4	3	13182.3
design_112	1	1.4	0	13280.3
design_113	1	1.4	-6	13522.5
design_114	1	1.4	-3	13382.3
design_115	1	1.4	-9	13691.7
design_116	1	1.5	3	13208.2
design_117	1	1.5	0	13259.5

design_118	1	1.5	-3	13382.2
Design No.	length	breadth	angle	Rw (N)
design_119	1	1.5	-6	13535.9
design_120	1.01	0.8	3	13123.4
design_121	1	1.5	-9	13687.5
design_122	1.01	0.8	0	13176.1
design_123	1.01	0.8	-3	13290.2
design_124	1.01	0.8	-6	13422.5
design_125	1.01	0.8	-9	13560.9
design_126	1.01	0.9	0	13133.3
design_127	1.01	0.9	3	13057.4
design_128	1.01	0.9	-3	13242.6
design_129	1.01	0.9	-6	13389.2
design_130	1.01	0.9	-9	13546.6
design_131	1.01	1	3	13004.1
design_132	1.01	1	0	13085.5
design_133	1.01	1	-3	13180.6
design_134	1.01	1	-6	13353.5
design_135	1.01	1	-9	13491.4
design_136	1.01	1.1	3	12972.4
design_137	1.01	1.1	0	13058.9
design_138	1.01	1.1	-3	13168.8
design_139	1.01	1.2	3	12963.1
design_140	1.01	1.1	-6	13310.5
design_141	1.01	1.1	-9	13490.1
design_142	1.01	1.2	0	13018.1
design_143	1.01	1.2	-6	13283.3
design_144	1.01	1.2	-3	13134.1
design_145	1.01	1.2	-9	13449.4
design_146	1.01	1.3	3	12915.4
design_147	1.01	1.3	-3	13127.8

design_148	1.01	1.3	-6	13297
Design No.	length	breadth	angle	Rw (N)
design_149	1.01	1.3	0	12991.5
design_150	1.01	1.3	-9	13459.8
design_151	1.01	1.4	3	12951.5
design_152	1.01	1.4	-6	13305.6
design_153	1.01	1.4	0	13006.3
design_154	1.01	1.4	-3	13131.9
design_155	1.01	1.4	-9	13515.2
design_156	1.01	1.5	3	12940.2
design_157	1.01	1.5	0	13024.9
design_158	1.01	1.5	-3	13136.4
design_159	1.01	1.5	-6	13337.6
design_160	1.02	0.8	0	12958.2
design_161	1.02	0.8	-6	13200.6
design_162	1.01	1.5	-9	13519.7
design_163	1.02	0.8	3	12874
design_164	1.02	0.8	-9	13406.5
design_165	1.02	0.8	-3	13069.4
design_166	1.02	0.9	3	12807.3
design_167	1.02	0.9	0	12890.2
design_168	1.02	0.9	-6	13161.9
design_169	1.02	0.9	-3	13005.5
design_170	1.02	0.9	-9	13334
design_171	1.02	1	3	12784.6
design_172	1.02	1	0	12845.8
design_173	1.02	1	-3	12967.6
design_174	1.02	1	-6	13118.5
design_175	1.02	1	-9	13321.8
design_176	1.02	1.1	-9	13306.9
design_177	1.02	1.1	3	12739.9

design_178	1.02	1.1	-3	12935.2
Design No.	length	breadth	angle	Rw (N)
design_179	1.02	1.1	0	12814.9
design_180	1.02	1.1	-6	13107.9
design_181	1.02	1.2	3	12743.4
design_182	1.02	1.2	0	12763.4
design_183	1.02	1.2	-3	12925.2
design_184	1.02	1.2	-6	13111.3
design_185	1.02	1.2	-9	13319.4
design_186	1.02	1.3	3	12718.1
design_187	1.02	1.3	0	12764.7
design_188	1.02	1.3	-6	13109.6
design_189	1.02	1.4	0	12812.7
design_190	1.02	1.3	-3	12928.7
design_191	1.02	1.4	3	12722.4
design_192	1.02	1.3	-9	13342.8
design_193	1.02	1.4	-3	12947.5
design_194	1.02	1.4	-6	13158.1
design_195	1.02	1.4	-9	13393.7
design_196	1.02	1.5	3	12746.7
design_197	1.02	1.5	0	12807
design_198	1.02	1.5	-6	13188.7
design_199	1.02	1.5	-3	12974.1
design_200	1.02	1.5	-9	13468.7

